Critical Review on Wax Deposition in Single-Phase flow

Charlie van der Geest[a,*], Aline Melchuna[b], Letícia Bizarre[a], Antonio C. Bannwart[c] and Vanessa C. B. Guersoni[a]

[a] *Center for Petroleum studies, University of Campinas, Campinas, São Paulo, Brazil*
[b] *Equinor - Rio de Janeiro, Brazil.*
[c] *School of Mechanical Engineering - University of Campinas. Campinas, São Paulo, Brazil.*

ARTICLE INFO

Keywords:
Wax Deposition
Waxy Crude Oil
Flow Assurance

ABSTRACT

Wax deposition is a costly problem for the O&G industry, especially for pipelines in cold environments. For at least three decades, the scientific community has overwhelmingly agreed that molecular diffusion is the main mechanism for wax deposition. There are, however, severe problems with models based on molecular diffusion. They rely on untested hypotheses and several empirical correlations; hence, they can hardly predict the experimental data from laboratory. For real fields, the prediction is no better than an educated guess - heuristic solutions. Several research areas in wax deposition need to be better understood, and these are discussed in detail here, with a highlight to the most important concern: the controlling mechanism. Is wax deposition indeed a mass transfer controlled phenomenon? What is the evidence supporting this "general knowledge"? Is it possible that, for some conditions, mass transfer is dominant, and for others, the phase transition mechanism is dominant? Apart from this main concern, we also promote discussions on other issues: the accuracy of empirical correlations for diffusivity, the behavior of crystals in the deposit and how that influences the general deposit behavior, non-Newtonian influence on heat transfer and mass transfer, among others. Wax deposition is a complex topic that has been reviewed over and over. In this review, however, we focus on both presenting what has been proposed and discussed in the literature and make a critical analysis on the topic. The goal is to increase the general knowledge by highlighting a number of gaps and challenges related to this complex and financially exorbitant issue.

Contents

*Corresponding author
ORCID(s):

1. Introduction

There are several open questions regarding wax deposition in pipelines. As a consequence, it is difficult to accurately predict where and how significant wax will accumulate in the production system. "Modern" simulators include various empirical parameters that are poorly explained or modeled [1]. The relevance of this general inaccuracy is the cost of removing or managing the deposit, which can represent the biggest OPEX of some fields [2].

Before we introduce the wax deposition process, it is important to briefly introduce the waxy crude oil fluid and its properties. As is widely-known, waxy crude oils are a complex mixture with a high concentration of high-molecular-weight linear alkanes (C_{18} upwards) [3]. From a thermodynamics perspective, the most important temperature for waxy crude oils, at least when discussing wax deposition, is the phase transition temperature. Even though there is experimental evidence that the Wax Dissolution Temperature (WDT) is the most accurate equilibrium solubility temperature [4], The literature mostly mentions Wax Appearance Temperature (WAT) due to the complexity of waxy crude oils. This review does not focus on this specific discussion; WAT is a meta-stable condition where wax crystals can be observed.

Figure 1 shows a general view of how the phenomena evolve for long enough pipelines, the coolant is represented as a schematic for a pipe-in-pipe system but, for this manuscript, it could be any sea current in any direction. As the oil flows in the pipeline, its average temperature decreases; when above the WAT, it is called hot flow regime [5]; when below the WAT, it is called cold flow regime [1, 6, 7]. As the oil flows in the cold flow regime, its composition changes because wax crystals precipitate. Hence, the characteristic temperatures also change downstream. The WAT or WDT

used throughout the manuscript always refers to the phase transition temperature, before the change in composition due to precipitation[8].

In Figure 1, the temperature profile is shown in red for two different regions. At the pipeline center (r=0), the bulk temperature is above the Wax Appearance Temperature (WAT) for the hot flow and, below the WAT, for cold flow condition. For the hot flow condition, as the radial position increases, the temperature decreases and reaches the WAT and the wax therefore starts to precipitate. As the radial position increases even more , the interface with the static deposit is reached and, at this point, we show a complex and non-continuous interface, which is the reality. For the cold flow condition, there is wax crystal precipitated in the bulk and, as the bulk is below the WAT, the interface is also below. Again, the phase transition temperature in the cold flow is no longer the original WAT since the composition of the fluid has changed.

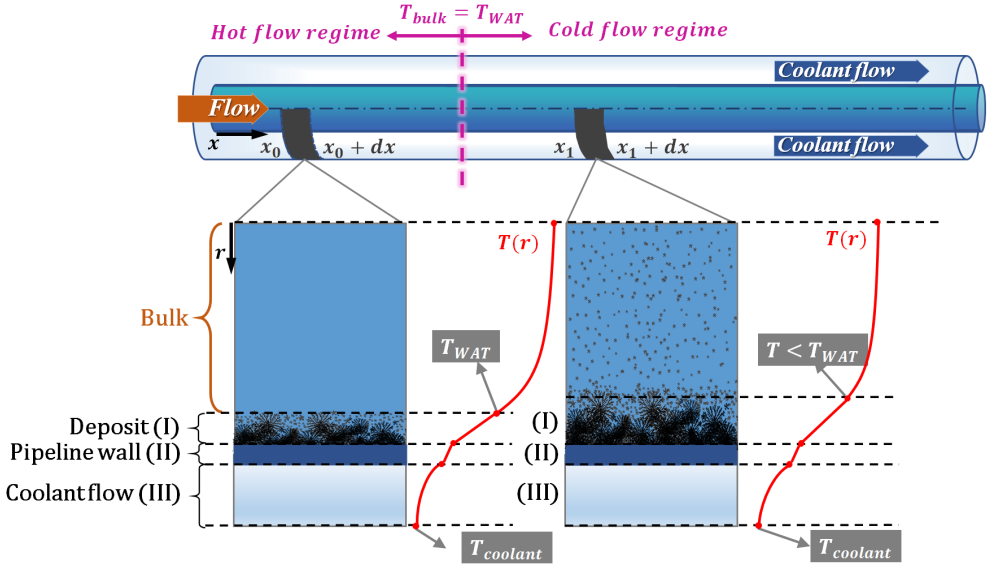

Figure 1: Schematic of wax deposition phenomena focusing on the transition between hot flow and cold flow.

The next discussion is the continuous and hydrodynamic smooth interface [1, 3, 9], and we highlight this assumption in Figure 2. The fractal dimension and crystalline growth (3D) are not considered and the solution is similar to the classic approach where the relative roughness of a pipe is disregarded. This hypothesis has not been verified for wax deposition and, to our knowledge, there are no experiments that quantify the effect of the relative roughness of the deposit. All models and commercial and academic simulators use the smooth and continuous hypothesis for the interface. Hence, from this point forward, when the interface is mentioned, we assume it is smooth and continuous.

It is important to separate the mechanism and the hypothesis for modeling each process during wax deposition. They are usually separated into three general areas: start, growth, and aging. The discussions in the literature mainly include the second and third problems [1, 3, 5, 10, 11, 12, 13, 14, 15, 16, 17, 18, 19]. Usually, the focus is on the kinetics of the deposit's thickness and how the concentration of the wax inside the deposit varies, assuming the deposit already exists.

A representation of a mass transfer approach focusing on growth and aging is represented in Figure 3, which shows a schematic of several phenomena during wax deposition. The arrows above the WDT show the radial direction of dissolved wax, the dissolved molecules are not represented. Wax particles are represented as black needles, however, the crystals' morphology varies considerably, their formats vary between needle-like, circular shape, and fractal crystals, depending on several conditions [20]. Molecular structure, cooling rate, shear stress, shear rate, temperature, and temperature histories are just some examples of variables that influence the morphology of crystals and agglomerates [21] [22].

In mass transfer-based models, the most accepted mechanism is molecular diffusion [10], [23], [14], [13]. In Figure 3, the temperature profile is shown in red. At the center of the pipeline (r=0), the bulk is above the WDT, thus no wax precipitated. As the radial position increases, the temperature decreases and reaches WAT and the wax starts

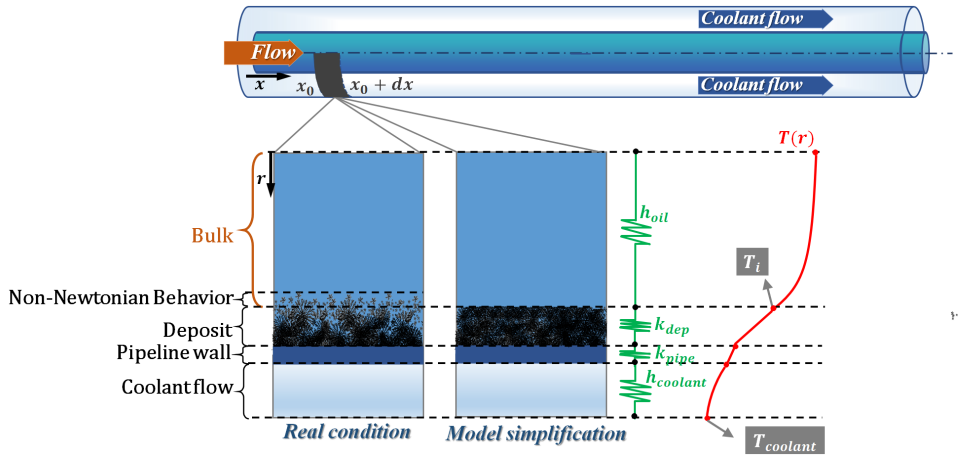

Figure 2: Schematic of the first simplification of every model, assuming a continuous and smooth interface.

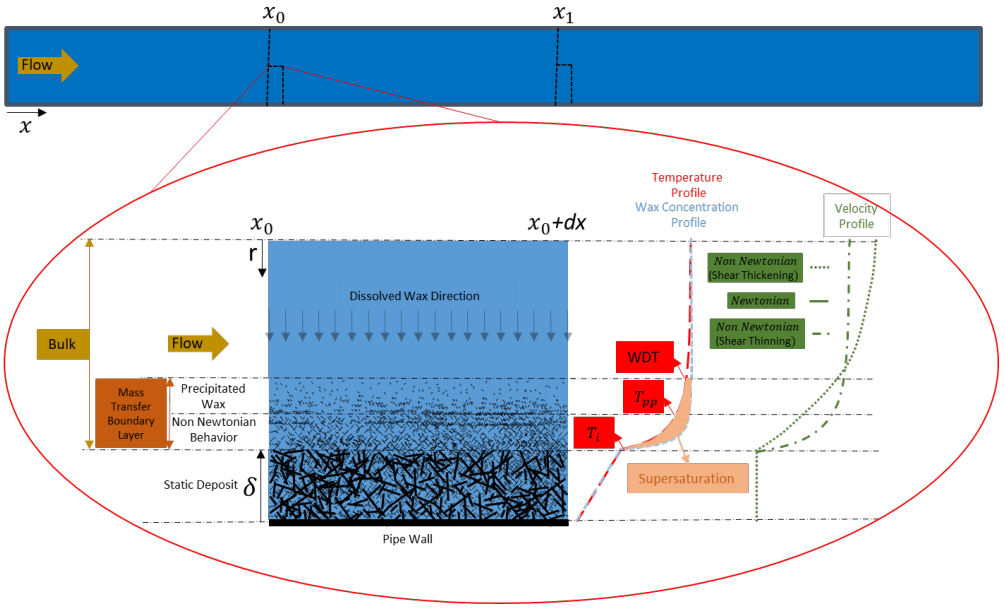

Figure 3: Schematic of mass transfer-based models for wax deposition phenomena in full complexity. Temperature, Concentration and Velocity profile possibilities.

to precipitate. As the radial position continues to increase, the pour point (T_{pp}) is reached, leading to a non-Newtonian behavior [24]. Further increasing the radial position, the interface with the static deposit is reached (T_i). Since Figure 3 is a representation of a mass transfer approach, the concentration gradient is also represented in blue. Supersaturation effects are represented by a discrepancy in the temperature profile and the concentration profile, this is based on the fact that the cooling down and the precipitation kinetics do not necessarily occur in the same time frame, meaning that the precipitation process can be longer than the cooling process, which leads to supersaturation [25].

Figure 3 also shows the velocity profile, considering several possibilities of non-Newtonian behavior, since that depends on the fluid and there is no consensus in the scientific community on the general behavior. One must highlight that most waxy crude oils have a shear thinning behavior when at constant temperature [26], [27]. However, if the viscosity increases because the temperature gradient is higher than the viscosity decrease, due to the shear rate gradient, the behavior of the crude would be similar to a shear thickening. Thus, both shear thickening and shear thinning are shown in the velocity profile.

From the interface all the way to the pipeline wall, a static porous media is represented. It is widely assumed that the thermodynamic properties are constant; *e.g.*, conductivity and specific heat, and a homogeneous radial distribution of mass [28]. The crystals were represented as needle-like, but again, a variety of morphologies have been observed. The average molecular weight of the deposit is known to increase over time, and that is the second main focus in the literature - the aging process [13, 16].

There are two main approaches in the literature on how to model wax deposition growth. The most accepted approach, mainstream modeling, is mass transfer based [3],[10], and the lesser known approach is what we shall call phase transition based [6]. Mass transfer models are based on the concentration difference between the bulk and the interface, usually assuming Fick´s first law. The phase transition model is based on partial freezing and phase transition from liquid to solid [19]. Both models use similar equations of heat transfer, the main difference between the two approaches is the boundary condition and what limits the growth of the deposit; the hypotheses shall be discussed in detail.

This review is separated into another nine sections. Firstly, a general view and the state of the art, followed by the energy conservation focusing on the hypotheses of the main approaches. After, an in-depth discussion of the mechanisms of the bulk assuming a Newtonian fluid. We then investigate how the literature discusses the effect of non-Newtonian behavior and how it can influence wax deposition assumptions and models. Once the bulk is covered, a discussion ensues on existing models and their hypotheses for the deposit. This is followed by a discussion on possible mechanisms for the beginning of the deposit. Finally, a brief description of the hypotheses and models presented in commercial and academic simulators. The conclusions include a summary of the main points.

2. General View: State of the Art

Once the problem has been introduced, a brief description of the state of the art regarding the approaches on wax deposition should help the reader navigate through the document. There are two main fronts in the state of the art on wax deposition discussion; one is applied by all commercial simulators and is accepted and used by most specialists. The other has a history of being overlooked by the literature, but has gained relevance in recent years due to the lack of predictability of the former. Both fronts shall be explained and discussed in detail in this manuscript.

Most of the literature regarding the second approach [6] calls it a heat transfer approach, but for clarity and because we believe this would better separate the models, this manuscript shall refer to it as phase transition approach, in short, they can be summarized as:

1. molecular diffusion + shear stripping [23]
2. phase transition (heat transfer) [6].

We start with a general perspective on the state of the art of these three mechanisms: mass transfer (molecular diffusion), shear phenomena (shear stripping), and heat transfer (phase transition). Clearly, it is not because these are the most discussed mechanisms in the literature that others are not present or important.

2.1. Molecular Diffusion + Shear Stripping

2.1.1. Mass Transfer Mechanisms: Molecular Diffusion

It is important to start the discussion on mass transfer mechanisms with the biggest problems of this approach. The main criticism regarding the mass transfer approach to wax deposition is the impossibility to predict the decrease in deposit size as the Reynolds number increases. To explain this occurrence, it demands another phenomenon related to the removal of mass from the deposit due to shear related phenomena. Although this is an interesting and seemingly appropriate hypothesis, there is a severe lack of direct experimental evidence of it. Despite the lack of evidence of its existence, there is almost no discussion on forces and mechanisms involved in the removal and no discussion on how the fracture occurs, whether a brittle fracture or a smooth removal, except for [29].

Another important point is that mass transfer models present a singularity at time equals zero (t=0). The user has to work around this singularity and mask it to make the model behave appropriately. The lack of proper initial conditions is definitely not a good sign and indicates a model based on weak physical principles.

Aside from these main issues, there are several others that lack answers when discussing mass transfer-based modeling. Most of them are subject of research by several groups, a few examples are: the effect of entropy and how it influences the mass transfer behavior due to supersaturation effects [25]; accuracy of Hayduk and Minhas [30] for complex fluids with molecules with more than 32 carbons; influence of precipitated molecules in the diffusivity of the

solute [31]; the effect of non-Newtonian behavior in mass transfer; and the influence of wax crystal size and fractal dimension in the rheological behavior and thus the deposition rate [32].

2.1.2. Shear Induced Based Mechanisms

The shear induced mechanisms in the literature of wax deposition were always secondary phenomena. They were always proposed as fitting-data phenomena, the only exception was Paso et al. [29]. Apart from this, they were not proposed based on fundamental laws and are extremely common in mass transfer-based literature [3] [13] [33]. The approach is usually to assume molecular diffusion and, if that is not enough, fit the data with shear induced mechanisms.

At the beginning of the research on the wax deposition, one mechanism was proposed to cause a positive net flow of precipitated particles between the bulk and the deposit, thus, causing an increase of the deposit: shear dispersion [9] [34]. After the review of Azevedo and Teixeira [9] and an abundance of experimental evidence [35] [36] [37], as properly described by Merino-Garcia et al. [1], the evidence showed that, as the shear rate increases, the size of the deposit decreases [35] [36] [37], thus, shear dispersion mechanism was no longer considered relevant.

Several other models and mechanisms were proposed to "predict" what was believed to be the effect of shear. Nowadays, the argument is that shear is responsible for controlling the size of the deposit [38] under high turbulent flows. Because they were always poorly defined secondary phenomena, the terms have been used broadly with different names and definitions. The detail of the models and approaches are described later in this review but, as discussed before, they are all based on empirical correlations that derive from the main assumption of mass transfer-based wax deposition model.

Venkatesan and Fogler [38], for example, called the phenomenon “shear reduction”, arguing this could either be the removal of mass from the deposit or hindering of the diffusion/flow of particles. Currently, it is more common to find what Venkatesan and Fogler [38] called “shear reduction” mechanism separated into two phenomena. The first and most famous being called “shear stripping” [39], which has also been called “shear sloughing” [29] [36], where the flow removes wax from the static deposit. The second mechanism, where the shear hinders the flow of particles towards the deposit, has been idealized but not properly described and formulated, and is referred to as “shear reduction” [39].

2.2. Phase Transition (Heat Transfer)

Because this is a less known and discussed approach in wax deposition literature, it is important to briefly describe it here. The main assumption of the phase transition approach is that the temperature of the interface is always constant and the wax deposition phenomenon would therefore be a phase transition problem; *i.e.*, a thermodynamics problem, similar to ice deposition of a single component [40]. A review on this approach has been published recently [6], where the discussion and hypothesis are presented in their entirety.

There are two strong arguments for phase transition-based models. First, all experimental data (small database) in the literature seems to indicate a constant temperature of the interface [16, 41, 42, 43, 44, 45, 46], and we highlight the recent measurements of Veiga et al. [41], which has the best measurements of the temperature profile in a wax deposition experiment in the open literature. Second, it can explain the fact that, as the Reynolds number increases, the deposit would be smaller, which is the biggest problem of mass transfer models. The heat transfer’s simple explanation (based on energy conservation) is that an increase in the Reynolds number decreases the convective thermal resistance, which in turn must be matched with a decrease in the deposit conductive thermal resistance via a decrease in the deposit thickness for the same temperature gradient.

A big problem with the hypothesis that the interface is always at WAT is the massive lack of comparison with experimental data, which is a direct consequence of the scientific community and *O&G* industry assuming molecular diffusion as dominant. To our knowledge, all experimental data compared to phase transition models were accurate, but obtained in small experimental apparatus, allowing reliable data, but severely limiting the phenomena involved. This is important to highlight, because the measurement of the interface temperature is probably the experiment that will prove what mechanism is dominant. To prove that wax deposition is indeed a molecular diffusion mechanism, some experiment needs to show that the temperature of the interface varies from the temperature of the wall to the WDT as the deposit grows.

The most important question arises here, which is: what limits the growth of the deposit, temperature or shear stress? One must note that there perhaps is no clear or simple answer to that. The size might be limited by both, depending on the conditions and fluids. It is certain that experimental campaigns focusing on testing the hypothesis

of both approaches are necessary.

3. Energy Conservation

The energy conservation is used by all wax deposition models. Most of the assumptions are similar regardless of being mass transfer or phase transition-based models. Some of those assumptions are not usually discussed in the wax deposition literature because they are "classic knowledge" but, since this is a review, we shall briefly present them. The interesting part is not the common assumption, but how the equations change as the assumptions of different models are made, which is why we decided to present the equations, as shown in the following sections. The discussion will start with the first control volume - the bulk. At this point, we assume the existence of a smooth continuous interface, which creates the frontier between the bulk and the deposit.

3.1. Bulk

Starting from a microscopic energy equation disregarding radiation and assuming constant thermal conductivity of the bulk (k_{bulk}):

$$\rho\left(\underbrace{\frac{\partial U}{\partial t}}_{storage}+\underbrace{\vec{u}\cdot\nabla U}_{convection}\right)=\underbrace{k_{bulk}\nabla^2 T}_{conduction}-\underbrace{p\overbrace{\left(\nabla\cdot\vec{u}\right)}^{\cong 0}}_{volumetric}+\underbrace{\overbrace{\vec{\vec{\tau}}:\left(\nabla\vec{u}\right)}^{\cong 0}}_{viscous\ dissipation}+\underbrace{S}_{source} \tag{1}$$

Where U is the internal energy of the bulk, p is pressure, τ is the tensor of stress, S is the source term, that is usually modeled as a phase transition term, ρ is the density, $\vec{u}$ is the velocity vector and ∇ is the Nabla operator.

By assuming the following:

1. incompressible fluid ($\nabla\cdot\vec{u}=0$)
2. constant pressure, thus, the internal energy is determined as a function of temperature applying the specific heat capacity ($\partial U = c_{p,bulk}\partial T$)
3. negligible viscous dissipation, as used in all wax deposition literature but with no discussion on its limitations, thus, we shall assume as true
4. similar bulk and wax density and no change in density when the wax precipitates in the bulk
5. axisymmetric flow
6. negligible re-circulation and secondary flow (not necessary when the solution is numeric)

And, finally, using cylindrical coordinates, we obtain [26]:

$$\rho c_{p,bulk}\left(\frac{\partial T}{\partial t}+u_x\frac{\partial T}{\partial x}+\overbrace{u_r\frac{\partial T}{\partial r}}^{\cong 0}\right)=k_{bulk}\left(\overbrace{\frac{\partial^2 T}{\partial x^2}}^{\cong 0}+\frac{1}{r}\frac{\partial}{\partial r}\left(r\frac{\partial T}{\partial r}\right)\right)+S \tag{2}$$

If the bulk is above the WAT (hot flow in the heat-transfer literature)[6], than the phase transition term is zero and it is possible to obtain the equation used by [26], a consensus in the literature. Lee [13] adds the momentum diffusion to this equation for turbulent flow with thermal diffusion, thus the assumption that it is constant is no longer valid and it should be kept inside the gradient of the temperature.

From this point forward, there are different approaches in the literature. Lee [13] argues that the heat generated by precipitation is around 0.1 % when compared with advection and diffusion term. They also disregarded the transient (storage) term in their simulations and assumed that the amount of mass precipitated in the bulk can be calculated using heat-mass transfer correlations. Mehrotra et al. [6] modeled the source term with the assumption that all the

latent heat released during precipitation is absorbed by the bulk.

$$\overbrace{\rho c_{p,bulk}\frac{\partial T}{\partial t}}^{Steady\ State\ =\ 0\ [13]} + \rho c_{p,bulk} u_x \frac{\partial T}{\partial x} = k_{bulk}\frac{1}{r}\frac{\partial}{\partial r}\left(r\frac{\partial T}{\partial r}\right) + \overbrace{\begin{cases} = 0 \quad T > WAT \\ k_r(C_b - C_{ws}) \approx 0\ [13] \\ \rho \Delta H \frac{\partial F_{w,bulk}}{\partial t}\ [6] \end{cases}}^{S} \tag{3}$$

If the solution of energy conservation of the bulk is not numeric, than more simplifications are necessary, integrating over the control volume considering the average velocity, integrating over length ∂x and radially ∂r, with some algebra and applying a classic boundary condition where the sub-laminar layer conduction and convection are assumed to be equal:

$$(A_i \Delta x)\rho c_{p,bulk}\frac{\partial T}{\partial t} + \dot{m} c_{p,bulk}\left(T(x_0,t) - T(x_1,t)\right) = (2\pi r)\Delta x \overbrace{k_{bulk}\frac{\partial T}{\partial r}\Big|_{r_i}^{-}}^{h(\bar{T}_b - \bar{T}_i)} + (A_i \Delta x)S \tag{4}$$

Lastly, the final form of the transient 1D average equation for the bulk as used by [6]. For clarity, we separate the areas with sub-indices: the flow area (A_i) and the superficial area of the interface (A_h). The temperature to calculate the radial heat transfer is the average between the points $\bar{T} = \frac{T(x_0,t)+T(x_1,t)}{2}$:

$$(A_i \Delta x)\rho c_{p,bulk}\frac{\partial T}{\partial t} + \dot{m} c_{p,bulk}\left(T(x_0,t) - T(x_1,t)\right) = A_h h(\bar{T}_b - \bar{T}_i) + (A_i \Delta x)S \tag{5}$$

Considering that the temperature at some radial position is below the WDT, thus assuming the presence of precipitated crystals [9], [29], [19], [11]; another diffusion-like mechanisms can occur, such as a Brownian diffusion [47]. Despite diffusion-like, several other mechanisms can cause radial transportation of wax, for instance, shear dispersion and gravity settling, all these mechanisms shall be discussed in detail in the next section and are unrestrained by the main model's assumptions.

Apart from all the mechanisms mentioned, there is the influence of precipitated crystals in the rheological behavior of the oil, non-Newtonian behavior [26]. There is a problem with this last topic as the influence regarding all phenomena that is non-Newtonian is not usually considered. The scientific community has limited knowledge of its influence on mass transfer, heat transfer and even the appropriate constitute equation. The few scientific publications that consider non-Newtonian behavior in wax deposition assume a viscoplastic constitutive equation [48], [24], [26] and, although that is a start, it is far from appropriate since no material only shows viscoplastic behavior. The topics related above evidence the complexity of the wax deposition study.

3.2. Deposit

There are several hypotheses that simplify the energy conservation equation that are valid for the bulk and the deposit, they shall not be discussed again as they are in section 3.1 for reference. The first hypothesis that is widely used by the models assumes that the deposit is static, thus the convection term shown in Equation 1 is zero $\vec{u}\cdot\nabla U = 0$. Assuming that the radial length scale is much smaller than the axial length scale, and also assuming that the density of the deposit and the bulk are similar,

$$\rho c_{p,dep}\frac{\partial T}{\partial t} = k_{dep}\nabla^2 T + \Delta H \overbrace{\frac{\partial(\rho_{dep}\bar{F}_{w,dep})}{\partial t}}^{\rho_{dep} \cong \rho_{bulk}} \quad \Leftrightarrow \quad \rho c_{p,dep}\frac{\partial T}{\partial t} = k_{dep}\left(\overbrace{\frac{\partial^2 T}{\partial x^2}}^{\cong 0} + \frac{1}{r}\frac{\partial}{\partial r}\left(r\frac{\partial T}{\partial r}\right)\right) + \rho \Delta H \frac{\partial \bar{F}_{w,dep}}{\partial t} \tag{6}$$

The next common assumption used by almost all the models is that the deposit is at thermodynamic equilibrium. Thus, it is possible to obtain [18]:

$$\rho c_{p,dep} \frac{\partial T}{\partial t} = k_{dep} \frac{1}{r} \frac{\partial}{\partial r} \left(r \frac{\partial T}{\partial r} \right) + \rho \Delta H \frac{\partial \bar{F}_{w,dep}}{\partial t} \tag{7}$$

Interestingly, most models assume, for simplicity, that the deposit is not at transient condition and therefore simplify them to steady state.

3.3. Interface (Heat Flux)

The last part of the heat transfer equation is the heat flux through the interface, which can be viewed as the boundary condition for the equations mentioned in sections 3.1 and 3.2. To highlight the difference between approaches, we show a classic example of both [5] and [3].

The most important difference is the definition of the boundary condition. Phase transition models always assume $T_i = WAT$. Mass transfer models do not impose a restriction in the temperature of the interface. Instead, they calculate the size of the deposit using diffusion and a series of empirical correlations and, with the value of thickness, it is possible to obtain the temperature of the interface with the equation below.

$$H = k_{dep} \left. \frac{dT}{dr} \right|_{r_i}^{+} - h_b \left(T_b - T_i \right) \quad \Leftrightarrow \quad H = k_{dep} \frac{\left(T_i - T_w \right)}{r_i \ln \left(\frac{r_i}{R} \right)} - h_b \left(T_b - T_i \right) \tag{8}$$

How to quantify the latent heat (H), the heat released by the mass that has solidified at the interface, is another important difference. Some mass transfer-based models use molecular diffusion-based correlations, while phase transition-based models assume that a new deposit will be generated with a homogeneous crystalline structure with ρ_{dep}, which is how they calculate the deposit's thickness.

$$k_{dep} \frac{\left(T_i - T_w \right)}{r_i \ln \left(\frac{r_i}{R} \right)} - h_b \left(T_b - T_i \right) = \begin{cases} \Delta H \rho_{dep} \bar{F}_{w,d} \frac{\partial r_i}{\partial t} \longrightarrow \textbf{Phase Transition-based model [5]} \\ \Delta H k_l \left(C_b - C_i(T_i) \right) \longrightarrow \textbf{Mass Transfer-based model [3]} \end{cases} \tag{9}$$

Again, the main difference is that the phase transition model assumes that the deposit interface temperature is constant and that all the heat lost due to the phase transition causes a homogeneous increase in the deposit, while mass transfer equations have no direct restrictions on the temperature of the interface. We highlight this again because this is most interesting. All experimental data of direct or indirect measurements of the interface temperature shows a constant value [16] [42][43], thus, all the evidence seems to direct us to the phase transition approach. The data is very limited and it is intriguing how the scientific community has taken little interest in this measurement. If the temperature of the interface is constant, then the mass transfer-based models are wrong, as shown in Equation 9, which is definitely an important open question in the literature.

4. Wax Deposition Mechanisms: Newtonian Fluid

The focus of this section is on the bulk, the wax that flows with the liquid phase, which is precipitated or dissolved. The net result from all the mechanisms defines the amount of mass deposited. First, a detailed discussion is provided on the mechanisms already presented *e.g.*: molecular diffusion, shear stripping, and phase transition. Then, a discussion is provided on all the other mechanisms that have been proposed by a long history of scientific investigations.

4.1. Molecular Diffusion

When modeling molecular diffusion of complex mixtures, there are two approaches: (a) the more complex thermodynamic approach, where the continuity conservation for each species is calculated [17]; (b) the average approach, where the species of wax are averaged, usually assuming that everything with more than 18 carbons is wax, and every species with less than 18 carbons is solvent. Once the solvent and solute are averaged, everything is treated as a binary

mixture [3]. The discussion in this section is based on literature that disregards the compositional thermodynamic modeling, *i.e.*, based on (b).

When assuming the average methodology, there are two different ways commonly used to model the mass transfer by molecular diffusion. First, considering thermodynamic equilibrium, which assumes that all molecules will precipitate immediately at their saturation temperature, this model has been called solubility model [13], and we call it the Equilibrium Model (EM) here [23]. This model is based on Fick's first law, with a noted simplification of assuming pseudo-steady-state [6].

Second is the model that uses heat transfer analogy to calculate mass transfer. This model has been called heat transfer analogy [13], we shall call it Film Mass Transfer model (FMT) [23]. This commonly uses several empirical correlations for heat and mass transfer. This model assumes that an infinite supersaturation can occur, since heat and mass boundary layer are completely independent. Lee [13] makes an interesting evaluation on the effects of supersaturation and the transition between both limiting cases.

An open question is how the supersaturation of wax in the crude can be quantifiable: *i.e.*, how the entropy of the system influences the amount of wax that can be dissolved in the oil at each condition. This has been addressed by a number of research groups [49]. The usual conclusion is that these two models are the upper (FMT) [10] and lower limits (EM) of molecular diffusion, if one considers that molecular diffusion is the only mechanism, those are the limits. But, as shown repeatedly, other mechanisms can influence the size of the deposit, thus, these boundaries should be treated carefully [39] [14].

The next discussion is the molecular diffusion coefficient. It is important because most research in the literature considers it a simple empirical correlation for wax in solvent mixtures for both model oil and real crude oil. We argue here that the inaccuracy of those models could lead to several misleading conclusions. Thus, it is clearly of major importance to understand how the molecular diffusion coefficient is measured, modeled, and often used in models throughout the industry and academy.

4.1.1. Molecular Diffusion Coefficient

The diffusion coefficient is different for each component of the fluid. Usually, the literature simplifies this to pseudo-components, being the solute, wax (C_{18} upwards), and the solvent, oil (C_{18} downwards). Most measurements and correlations for diffusion coefficient were obtained assuming the hypothesis of binary mixtures. Hayduk and Minhas [30] measured the diffusion coefficient for paraffin solutes in paraffin solvent, then they fitted a correlation (arguably had a 3.5% error), which is used by most of the models based on molecular diffusion [3, 13, 17, 23, 27, 50] and represents a scientific step forward for hydrocarbons. The industry and academy overwhelmingly use either Hayduk and Minhas [30] or similar empirical correlations such as Wilke and Chang [51].

There is a problem with this type of empirical correlation [52]; they are dimensionally incorrect, which most likely means that they are accurate for a limited set of conditions, however, the accuracy and conditions are never discussed in the wax deposition literature. Nevertheless, these empirical correlations are vastly used for all kinds of oils in all conditions. Sousa and Matos [52] discussed a correction of Hayduk and Minhas [30]correlation, which had a typographical error that consequently impacted several works of experimental comparison presented in the literature.

$$D_{wo} = 13.3\ 10^{-8}\ \frac{T^{1.47}\mu^{\gamma}}{V_A^{0.71}} \tag{10}$$

$$\gamma = \frac{10.2}{V_A} - 0.791 \tag{11}$$

Another correlation to calculate the diffusion coefficient was proposed for more generic purposes by Wilke and Chang [51], and has also been used in the literature for wax deposition. Wilke and Chang [51] correlation was fitted for a bigger range of fluids, not only hydrocarbons, and a broader set of conditions.

$$D_{wo} = 7.4\ 10^{-8}\frac{\left(\varphi M_o\right)^{0.5} T}{\mu V_A^{0.6}} \tag{12}$$

There are several experimental procedures to obtain the diffusivity coefficient: NMR [53, 54, 55], Taylor dispersion method [56, 57, 58], unsteady-state porous frit [59], digital holography interferometry [60, 61], and a Teflon-based T-shaped microfluidic chip [62]. Some authors [63, 64] developed a collection of work with data from the experimental diffusivity coefficient for different components, which enabled the comparison between different methodologies for the same component.

Mutina and Hürlimann [55] measured the diffusivity applying the RMN technique and showed that the diffusivity *vs.* relaxation time is a surface for real crude oils. That is known and well understood because several solutes are present in the system and each solute has a different diffusion coefficient. The importance of such measurements is that, compared to Hayduk and Minhas [30] predictions, the average error can be 50% higher. It is important to highlight that Mutina and Hürlimann [55] did not show the viscosity with temperature, thus only a small part of their dataset was compared to the correlation of Hayduk and Minhas [30].

As a highlight, the evidence revealed by Leahy-Dios and Firoozabadi [63] and Mutina and Hürlimann [55] showed that just applying the correlation from Hayduk and Minhas [30] can lead to high error in diffusivity prediction, especially when dealing with real waxy crude oils, where several important effects are disregarded: asphaltenes, non-Newtonian behavior, among others. But, even for controlled solutes and solvents, there is evidence [63] that Hayduk and Minhas [30]is considerably higher than 3.5%.

4.1.2. Limits of Molecular Diffusion

The FMT model assumes that there is no precipitated wax in the bulk. The EM model assumes that all the precipitated crystals outside the vicinity of the static deposit flow with the bulk and do not become part of the deposit. This is shown in Figure 4 by leaving a crystal-free space in the vicinity of the interface. It is also shown that the FMT-based model does not have a mass transfer boundary layer, since it assumes infinite supersaturation, thus, no wax crystal precipitate.

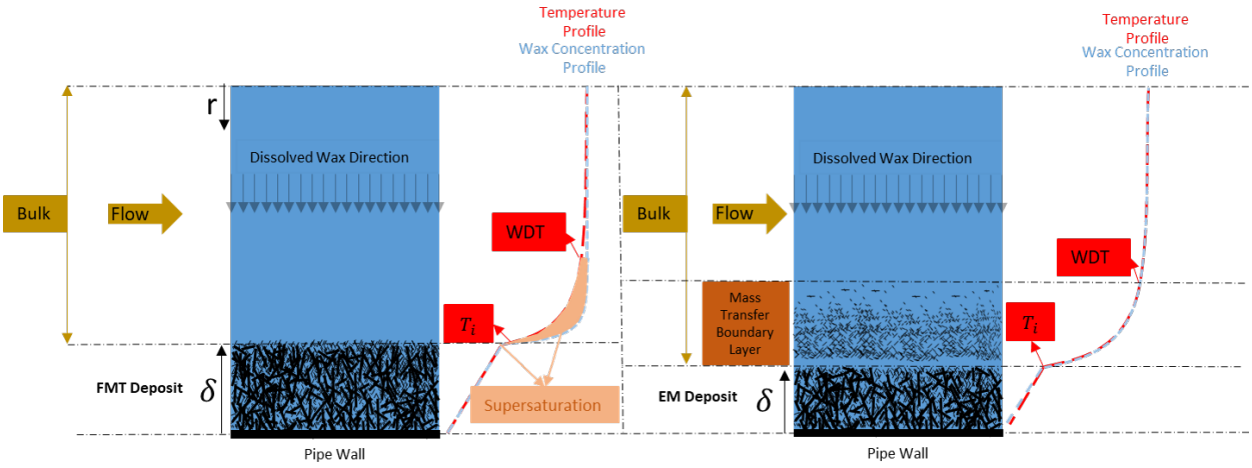

Figure 4: Schematic of the difference between EM and FMT models

4.1.2.1 Equilibrium Model:

There are three variables that need to be determined in order to calculate the total mass transferred through this mechanism: the molecular diffusion coefficient (D_{wo}), the concentration gradient $\left(\frac{dC}{dr}\right)$, and the temperature gradient $\left(\frac{dT}{dr}\right)$. The main assumption is that there is a thermodynamic equilibrium in the mass transfer boundary layer.

$$\dot{m}_{md} = (2\pi r L)\, D_{wo}\, \frac{\partial C}{\partial r} = (2\pi r L)\; D_{wo}\, \frac{dC}{dT}\bigg|_{T_i} \frac{dT}{dr}\bigg|_{r_i}^{-} \tag{13}$$

In Equation 13, D_{wo} , the molecular diffusivity of wax in oil $\left[\frac{m^2}{s}\right]$ is usually calculated using correlations such as Hayduk and Minhas [30], and both temperature and concentration gradients are obtained at the interface. The concentration gradient $\left(\frac{dC}{dT}\right)$ is calculated based on the temperature of the interface. It is obtained from the solubility curve of the oil, usually measured in DSC, and an example of a solubility curve is shown in Figure 5. The concentration gradient is the derivative of the solubility curve.

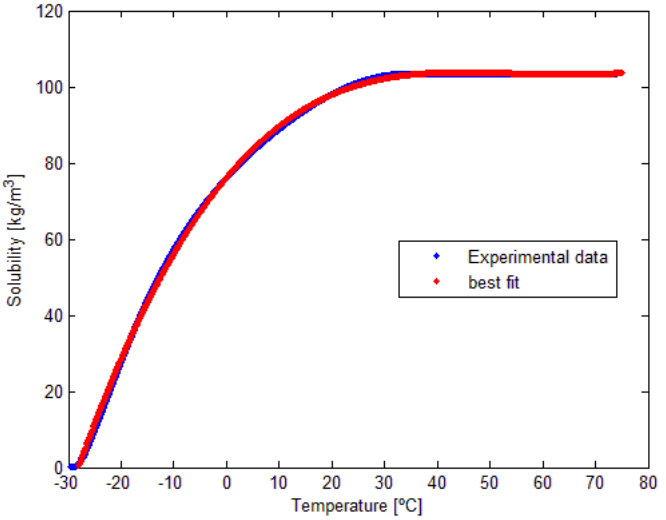

Figure 5: Solubility of a waxy crude oil [14]

The temperature gradient $\left(\frac{dT}{dr}\right)$ is obtained at the bulk side, in the vicinity of the interface, it is usually calculated using the convection equation. The temperature gradient $\left(\frac{dT}{dr}\right)$ can be obtained by solving 2D heat transfer calculation, as all commercial and academic simulators do, which is previously discussed in Section 3.1, or by using empirical correlations for Nusselt numbers [13] assuming steady state heat transfer

$$\left.\frac{dT}{dr}\right|_{r_i}^{-} = \frac{Nu\left(T_b - T_i\right)}{-2r_i} = \frac{h\left(T_b - T_i\right)}{k_{oil}} \tag{14}$$

4.1.2.2 Film Mass and Transfer (Heat Analogy)

This approach has been called differently in the literature but, in this review, the term Film Mass and Transfer (FMT) will be used. The heat transfer and mass transfer equations are completely independent. The heat transfer boundary layer does not interact with the mass transfer boundary layer. This is relevant in cases where the precipitation kinetics is slow, thus supersaturation is maximum [11]. This model was proposed by [3] [10].

As has been discussed by several studies [23] [38] [13], in the FMT model, supersaturation is maximum. This is a common phenomenon when cooling down complex fluids. This basically happens because the rate of temperature change is faster than the rate of precipitation of wax, thus the fluid stays at a meta-stable configuration, until equilibrium is reached, and the phase transition occurs.

$$\dot{m}_{md} = (2\pi r L)\, k_M [C_b - C_i(T_i)] \tag{15}$$

where k_M is the mass-transfer coefficient, it can be calculated either by empirical correlations, assuming heat and mass transfer analogy, or by numerical simulation, based on the Sherwood number (Sh). By numerically solving the

mass conservation of the system, it is possible to calculate the concentration gradient and, consequently, the mass transfer coefficient.

$$Sh = \frac{(-2r_i)\left.\frac{dC}{dr}\right|_{r_i}^{-}}{[C_b - C_i(T_i)]} = \frac{k_M(2r_i)}{D_{wo}} \tag{16}$$

The method to obtain the mass transfer coefficient is based on dimensionless correlations for the Nusselt and Sherwood numbers. There are several proposed empirical correlations for obtaining the Nusselt and Sherwood numbers. There are recent reviews on correlations for laminar flow [65] and on general heat transfer correlations for single phase flow [66]. The most common ones used in the literature of wax deposition are shown in Table 1. The correlation from Gnielinski [67] is the most accurate for turbulent flow and the correlation from [68] is the most used for wax deposition calculations. It is important to highlight that none of these correlations consider non-Newtonian behavior, all empirical correlations were fitted for model fluids in controlled conditions for Newtonian fluids.

Table 1
Complementary heat and mass transfer correlation widely used in the Petroleum industry

Hausen [69]		Limits
Nusselt (Nu)	$3.66 + 0.0017813\frac{Gz^{\frac{5}{3}}}{\left(1+0.04(Gz)^{\frac{2}{3}}\right)^{0.5}}$	$Re < 2000$ $Pr < 12 \times 10^3$ $Gz < 100$
Sherwood (Sh)	$3.66 + 0.0017813\frac{Gz^{\frac{5}{3}}}{\left(1+0.04(Gz)^{\frac{2}{3}}\right)^{0.5}}$	
Sieder and Tate [70]		
Nusselt (Nu)	$1.86\ Gz^{\frac{1}{3}}\left(\frac{\mu}{\mu_w}\right)^{0,14}$	$Re < 2000$ $Pr < 12 \times 10^3$ $Gz > 100$
Sherwood (Sh)	$1.86\ Gz^{\frac{1}{3}}\left(\frac{\mu}{\mu_w}\right)^{0,14}$	
Gnielinski [67]		
Nusselt (Nu)	$\frac{\frac{f}{8}(Re-1000)\,\mathrm{Pr}}{1+12.7\left(\frac{f}{8}\right)^{0.5}\left(\mathrm{Pr}^{\frac{2}{3}}-1\right)}$	$3000 < Re < 5\ 10^6$ $0.5 < Pr < 2\ 10^3$ $\frac{L}{d} < 60$
Sherwood (Sh)	$\frac{\frac{f}{8}(Re-1000)Sc}{1+12.7\left(\frac{f}{8}\right)^{0.5}\left(Sc^{\frac{2}{3}}-1\right)}$	
Chilton and Colburn [68]		
Nusselt (Nu)	$0.023\ Re^{0.8}\ Pr^{\frac{1}{3}}$	$Re > 2000$ $Pr < 12\ 10^3$ $\frac{L}{d} > 60$
Sherwood (Sh)	$0.023\ Re^{0.8}\ Sc^{\frac{1}{3}}$	

4.1.3. Supersaturation in Molecular Diffusion

WDT is closer to the equilibrium state [19] [11], the difference between WAT and WDT is that, during WAT measurements, the system is at meta-stable condition. Ravichandran [49] showed that supersaturation indeed occurs by comparing high temperature gradient with low temperature gradient solubility curves in DSC. The supersaturation phenomenon occurs because the entropy of solid wax is higher than liquid wax, some degree of supersaturation is mandatory for precipitation to occur [71].

$$\frac{dC}{dt} = k\left[C - C_{eq}\right]^a \tag{17}$$

There are several approaches in the literature to model the saturation level of waxy crudes [47]. In wax deposition literature, as shown by Ravichandran [49], it is common to apply the supersaturation ratio (S_s), a correction factor for the supersaturation in both the boundary layer and interface. Ravichandran [49] defined it as the concentration available for deposition by the equilibrium concentration. S_s is always higher than 1, which means that less mass would be transferred to the deposit, when compared with the infinite supersaturation, which is what the FMT theory suggests.

$$\dot{m}_{md} = (2\pi r L)\ k_M[C_b - S_s C_i(T_i)] \tag{18}$$

4.2. Shear Stripping and Sloughing Mechanism

Shear stripping and sloughing are the same mechanisms with different methodologies to quantify the amount of wax removed. The most common is by fitting experimental data assuming shear stripping and diffusion are the only mechanism [72] [31] [38]. Paso et al. [29] held a more physically grounded discussion of the possible removal mechanism. They described three possible fracture models and, for one of them, they derive an equation for the tensile fracture, to remove part of the deposit, the stress (τ_c) should be proportional to the deposit's elastic modulus (E) and the intrinsic fracture Energy (G).

$$\tau_c \propto \sqrt{EG} \tag{19}$$

The term sloughing mechanism has been used in wax deposition at least since Weingarten and Euchner [36]. They argued that when the stress, due to shear, was big enough to overcome the strength of the wax deposit, sloughing would occur. They did not attempt to model or quantify the sloughing mechanism.

Matzain [31] and Venkatesan and Fogler [38] took different approaches when trying to model the shear stripping mechanism. They both had experimental evidence that the size of the deposit decreased as the shear rate increased, evidencing that shear dispersion should not be playing a major role. They, however, did not directly observe any radial displacement or removal but, as the Reynolds number increased, and the thickness was smaller, they assumed that a shear stress related phenomenon was removing wax.

Figure 6 shows a representation of the shear stripping phenomena. It is important to highlight that if shear stripping is controlling the upper limit of the deposit's thickness, it must occur throughout the deposit. As the deposit increases, the velocity of the fluid also increases. Therefore, the bigger the deposit, the bigger the shear stripping effect. In Figure 6 shows the decrease in the deposit thickness due to shear stripping, assuming that there are only two mechanisms involved in wax deposition; molecular diffusion and shear stripping. Models for shear stripping are shown in Table 2 and described below.

To consider the shear stripping effect, Matzain [31] proposed an adjustment equation for the Reynolds number. As the modified Reynolds number increases, the shear stripping parameter increases. By inversely multiplying the shear stripping factor (Π_2) to the mass diffusion model, the amount of mass deposited decreased.

Venkatesan and Fogler [38] proposed a shear stress-dependent model by fitting empirical parameters using a series of experimental data. Thus, they assumed that the overestimation calculated by molecular diffusion either did not become part of the deposit or was stripped away.

Ramirez-Jaramillo et al. [72] performed a simulation applying a compositional model (modified from Svendsen [73]). They used the term shear removal instead of shear stripping and their innovation was to assume shear stripping is proportional to the mass of the deposit (M), not only the shear stress. As in every other attempt to model shear stripping, they used two empirical parameters.

Merino-Garcia et al. [1] described a set of experimental conditions evidencing that the shear stripping effect rather than shear reduction should be considered as the main mechanism after the molecular diffusion. They argued that the shear stripping effect should be calculated from a function of shear rate.

Correra et al. [33] considered the shear stripping effect by calling it the ablation effect. They added a term for the consistency of the deposit (ψ), which is a function of the aging effect. They also used one empirical coefficient.

Wang et al. [74] used the model proposed by Burger et al. [34] for shear dispersion mechanism (Table 3) and applied a poorly-defined concept of shear energy (E_s), using it to calculate the total flux due to shear phenomena. The value of total flux due to shear, minus the shear dispersion provided the shear stripping flux. They applied more

empirical constants than usual for this kind of study.

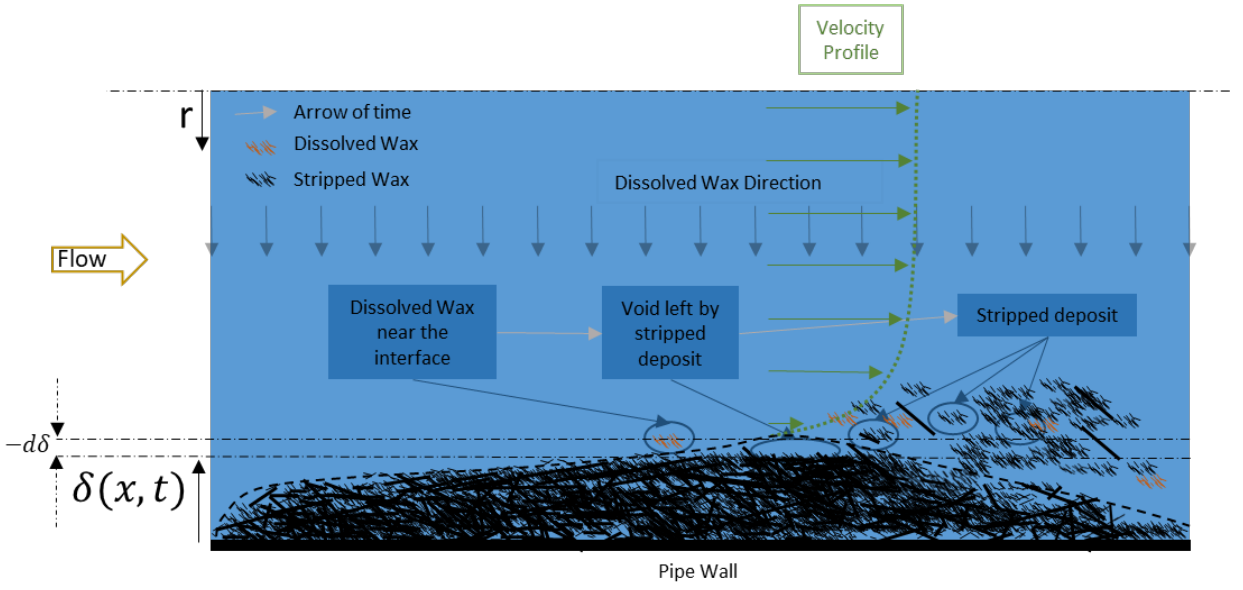

Figure 6: Schematic of the shear stripping phenomena, focusing on Mass transfer-based mechanisms

Table 2
Shear Stripping Models

Authors	Model	Empirical Parameters
Matzain [31]	$\Pi_2 = 1 + a_{Mat} Re_M^{b_{Mat}}$	$a_{Mat},\ b_{Mat}$
Venkatesan and Fogler [38]	$\dot{m}_{ss} = a_{Ven}\ \tau^{b_{Ven}}$	$a_{Ven},\ b_{Ven}$
Ramirez-Jaramillo et al. [72]	$\dot{m}_{ss} = a_{Ram} M\ \tau e^{\frac{b_{Ram}}{T_i}}$	$a_{Ram},\ b_{Ram}$
Merino-Garcia et al. [1]	$\dot{m}_{ss} = a_{Mer}\ A\ f(\dot{\gamma})$	a_{Mer}
Correra et al. [33]	$\dot{m}_{ss} = a_{Cor}\ A\ \frac{1}{\psi}\ \lvert\tau_n\rvert$	a_{Cor}

4.3. Phase Transition

Regardless of the hypothesis and models, the wax deposition phenomena is always related to heat transfer. Each model hypothesizes how the static deposit will stop growing, or how it will age, but there are always heat transfer equations involved. In this section, the interest only lies in presenting the hypothesis of phase transition-based models [6], those that assume that the interface is at a constant temperature, which in turn assume that wax deposition is a phase-transition phenomenon and not a mass transfer phenomenon.

This approach argues that the wax deposition process is similar to ice deposition. Interestingly, Ehsani and Mehrotra [40] have shown that the same set of equation and hypothesis could be used to model experimental results for water solidification (ice formation), a single component with no diffusion, and multi-component waxy crude oil, showing further evidence that wax deposition might be a phase transition phenomenon. In the literature, this approach is usually separated into steady state and transient approaches, so we shall present it following the same idea.

4.3.1. Steady State

Based on the notation shown in Figure 3, assuming there is a significant increase in temperature between the axial position x_0 and x_1, the heat flux through the entire pipeline system is classically defined as [75]

$$q = \dot{m}_{bulk} C_{bulk} (T_b(x_0) - T_b(x_1)) = U_{total} A (T_b - T_c) \tag{20}$$

Where T_b and T_c are the temperature of the bulk and coolant, $c_{p,bulk}$ is the specific heat capacity of the fluid. For the general heat transfer, the boundary and initial conditions depend on the desired experimental set-up solution [76] [18]. Assuming a deposit exists, a classic representation of the thermal resistance can be applied, resulting in four resistances. The upper letter R represents the fixed size of the pipeline, being R_{in} the inner radius and R_o the outer radius of the pipeline. The lower letter r_i represents the radius of the interface, which is $r_i(x,t) = R_{in} - \delta(x,t)$, thus, a function of time and the axial position.

$$\frac{1}{U_{total}} = \frac{1}{h_{oil}} + \frac{\overbrace{R_{in}\ln\left(\frac{R_{in}}{R_{in}-\delta}\right)}^{R_{in}\ln\left(\frac{R_{in}}{R_{in}-\delta}\right)}}{k_{dep}} + \frac{R_{in}\ln\left(\frac{R_o}{R_{in}}\right)}{k_{pipe}} + \frac{1}{h_{coolant}} \tag{21}$$

4.3.2. Transient

For the transient solution, the detailed discussion is shown in Section 3.1. A simplified model for the energy conservation for the bulk is: the total energy loss by the bulk equals the heat transferred to the deposit through convection in addition to the increase in the average temperature of the volume of the bulk [5].

$$(A_i\Delta x)\rho c_{p,bulk}\frac{\partial T}{\partial t} + \dot{m}c_{p,bulk}\left(T(x_0,t) - T(x_1,t)\right) = A_h h(\bar{T}_b - \bar{T}_i) + (A_i\Delta x)\rho\Delta H\frac{\partial F_w}{\partial t} \tag{22}$$

The final energy conservation for the deposit is shown below and the entire derivation of such equation is shown in 3.2. This is a strong differentiation from phase transition-based models and mass transfer-based models, since mass transfer-based models seldom assume a transient deposit. From Equation 7 and assuming thermodynamic equilibrium,

$$\overbrace{\frac{\rho c_{p,dep}}{k_{dep}}}^{\alpha^{-1}}\frac{\partial T}{\partial t} = \frac{1}{r}\frac{\partial}{\partial r}\left(r\frac{\partial T}{\partial r}\right) + \frac{\rho_{dep}\Delta H}{k_{dep}}\overbrace{\frac{\partial \bar{F}_{w,dep}}{\partial T}}^{Equilibrium}\frac{\partial T}{\partial t} \tag{23}$$

$$\frac{1}{r}\frac{\partial}{\partial r}\left(r\frac{\partial T}{\partial r}\right) = \left(\frac{1}{\alpha} - \frac{\rho_{dep}\Delta H}{k_{dep}}\frac{\partial \bar{F}_{w,dep}}{\partial T}\right)\frac{\partial T}{\partial t} \tag{24}$$

The last part of the heat transfer modeling, heat flux through the interface, is the boundary condition already shown in Equation 8. Again, the most important assumption of phase transition-based models is the constant boundary: the temperature at the interface is always constant.

4.4. Soret Diffusion

Soret diffusion, also named thermal diffusion, refers to the mechanism that has the temperature gradient as a driving force for the wax deposition [77]. This occurs because the temperature gradient causes mass (light and heavy wax) separation in the oil phase. Some authors have argued that the Soret diffusion effect is negligible [1], others stated that it is necessary to consider it for a correct assessment of the wax deposition problem [78]. There is no evidence in the literature that Soret diffusion has any effect on wax deposition.

4.5. Gravity Settling

Gravity settling has been disregarded in many studies because there is evidence of homogeneous deposit in vertical pipelines. There are, however, recent studies for horizontal flow in bigger pipelines, when the bulk is below the WDT, which appear to have deposit only at the bottom when under positive heat flux, meaning no molecular diffusion. This study could indicate that, in some conditions, the gravity settling should not be disregarded [79]. However, there is a lot of evidence [14, 16, 34, 80] that, for single phase flow, there is no difference on the deposit's thickness radially, thus, these results should be better understood.

4.6. Solubilization of wax

By this mechanism, the size of the deposit would be controlled by wax solubilization at the interface, when the deposit's thickness increases and reaches a point closer to the WDT, the wax crystals at the interface would start to solubilize in the bulk and flow with the stream. This is considered in a few commercial simulators [81]. This is classified as a mass transfer-based mechanism, because it is modeled as a solubilization mechanism and not as a phase change between the solid deposit to a liquid bulk. Regardless of its classification, the results of the prediction are similar, because this occurs at WDT, and if the deposit were modeled as a heat transfer mechanism, there would be no deposit, since the temperature of the interface is assumed constant at WAT, which shall be explained in detail below [82].

4.7. Enthalpy-porosity approach

Banki et al. [78] proposed a model for laminar flow based on the thermodynamics of irreversible processes that do not require applying the chain rule to decouple concentration gradient with temperature gradient, as shown in Equation 13. In other words, they proposed a solution for the wax deposition problem in a way similar to the one described in the phase transition-based model [6]. For this, they used the enthalpy-porosity formulation, a special approach to solve moving boundary / Stefan problems [83].

In the work of Banki et al. [78], the authors assumed the precipitation of wax leads to a gel that can be modeled as a pseudo-porous medium by a Darcy-type equation. The energy equation for the two-phase flow is written in terms of enthalpy instead of temperature (Section 4.3). They showed that the molecular and thermal diffusion can be considered together, but a consistent formulation is needed without replacing the concentration gradient with the temperature gradient (chain rule application - common in mass transfer-based model), otherwise, incorrect results can be obtained. This approach [78] has since then been extended to turbulent flow by Albagli et al. [84].

4.8. Brownian Diffusion

For this mechanism, we consider that the precipitated wax molecules collide randomly with the bulk molecules, this kind of random collisions cause a random Brownian motion of the suspended particles. The collisions tend to homogenize the distribution of precipitated particles throughout the bulk [47]. At the interface, the concentration due to random flow is zero because the particles are static, thus, there is a concentration gradient of precipitated particles, which is the argument for considering Brownian diffusion as relevant to deposition, as discussed by Azevedo and Teixeira [9].

$$\dot{m}_{bd} = A_i D_{bd} \frac{dC}{dr} \tag{25}$$

There is considerable evidence of no radial displacement of wax particles, the recent work of Cabanillas et al. [28] has shown no radial displacement of precipitated wax particles. The work of Hamouda and Davidsen [37] also showed no lateral displacement when the pipeline was divided into three sections with different boundary conditions. This is evidence that neither shear dispersion nor Brownian diffusion are relevant.

Ehsani et al. [85] evaluated the effect of suspended wax crystals in wax-solvent mixtures on the solid deposition process in the cold flow regime. The results obtained with the filtered and unfiltered mixtures under turbulent conditions concluded that the suspended wax particles do not affect the deposit mass or thickness in the cold flow regime.

There are models to calculate the Brownian diffusivity coefficient but, as shown by Cabanillas et al. [28], Hamouda and Davidsen [37], and Ehsani et al. [85], no radial movement of wax crystal has been observed toward the deposit, so it appears that Brownian diffusion could be disregarded. For this reason, there is no point in diving into the methods of calculating the Brownian diffusion coefficient.

4.9. Shear Dispersion

The shear dispersion mechanism occurs because there is a net transport of mass when several particles are flowing near each other under different shear conditions. In the interface, there is a high shear. In the middle of the bulk, there is low shear and high velocity. This velocity gradient causes the particles to rotate and, consequently, a rotational flow at the vicinity of each particle. This secondary flow causes a drag in the particles nearby, generating, on average, a net flow of particles toward the deposit [34].

An important point that should be briefly addressed; due to the difficulties in observing the radial movements of wax crystals, the work of Burger et al. [34], and all those based on his studies, made a mix of shear dispersion and Brownian diffusion, this problem was described by Azevedo and Teixeira [9] and Merino-Garcia et al. [1]. The problem is that when everyone stopped considering shear dispersion as relevant, they basically stopped considering Brownian diffusion as relevant, due to the confusion generated by the methodology of Burger et al. [34]. This misconception can still be seen in recent studies such as Wang et al. [74]. The shear dispersion mechanisms are shown in (Table 3).

Fasano et al. [47] proposed a shear dispersion model based on the shear stress (τ_n) applied to the deposit surface with normal $\vec{n}$ and the concentration at the interface (Table 3). This model is interesting because, despite considering shear dispersion, it considers the effects of the concentration of aggregated (C_a) and non-aggregated (C_n) wax crystals differently.

Table 3
Shear dispersion models

Authors	Model	Empirical Parameters
Burger et al. [34]	$\dot{m}_{sd} = a_{Bur}\ A\ C_w\ \dot{\gamma}$	a_{Bur}
Fasano et al. [47]	$\dot{m}_{sd} = -\left(a_{Fas}\ \lvert\tau_n\rvert\ C_a - b_{Fas}\ \lvert\tau_n\rvert\ C_n\right)\ \vec{n}\cdot A$	$a_{Fas}; b_{Fas}$

4.10. Shear Reduction

The meaning of this term has shifted quite significantly. Venkatesan and Fogler [38] used the term in a general perspective meaning anything related to shear that could decrease the final thickness, either by removal of mass from the deposit or by hindering the diffusion/flow of particles to the deposit. As the definition of shear stripping or shear sloughing improved, the term shear reduction has become vaguer. Recently, shear reduction has been referred as some phenomenon caused by shear that hinders the flux of particles towards the deposit. It has no physical explanation, no proper description, and no formulation [39].

5. Non-Newtonian Behavior

The influence of rheology in wax deposition problems has recently been a common topic in the scientific community, and it is now clear that one of the next frontiers on wax deposition understanding and modeling is related to rheology. Therefore, there is a need to understand and better investigate non-Newtonian influence in wax deposition. In general, there are few studies on the influence of rheological behavior on wax deposition-related problems [24][26][47][86].

There are studies on how viscoplastic materials influence momentum conservation through classic friction factor analogies [48][87]. When discussing the influence of rheology in the wax deposition, most studies use simplified viscoplastic constitutive equations, such as Herschel Buckley [24][26], power law or Bingham [47][86]. This is clearly a step forward, but there are no studies showing the influence of more complex rheological behavior, such as elasticity or thixotropy. This is relevant because there is plenty of evidence that waxy crude oils present such behaviors at low temperatures [14][87][88][89].

When assuming a non-Newtonian behavior, the first simplification is the most common in fluid mechanics, which is the continuous hypothesis. All phenomena involved with precipitated crystals in the bulk, which is what caused the non-Newtonian behavior, are treated in the macroscopic form - constitutive equation. This is important because, as everything involving wax deposition, the complexity is slightly higher. When there is a phase in suspension, the continuous assumption poses limitations, the system is actually a colloidal system, with stability dependence on the precipitated particle distribution, their morphology, and several other parameters. The reason why this is usually a sound hypothesis is because, when the system is flowing, shear related forces stabilize the colloidal system, but the limitations of those assumptions for the specific case of wax deposition are not well documented.

In the last section, due to historical and reviewing perspectives, all the mechanisms associated with wax deposition were presented. Over time, as scientific knowledge increased, some of those mechanisms proven to be irrelevant, with no contribution to wax deposition [49]. From this point on, the effects of non-Newtonian behavior on the most accepted approaches will be discussed.

Even the most recent studies that investigate the influence of non-Newtonian behavior on wax deposition fail to discuss the influence on diffusion coefficient (D_{wo}). This is relevant because the diffusion coefficient formulations, as have been discussed in the Newtonian section, were proposed for binary solutions of Newtonian fluids. There is considerable evidence that the accuracy of equations like Hayduk and Minhas [30] decreases as the complexity of the fluid increases. This could be even worse when the fluid has non-Newtonian behavior [90].

At the vicinity of the interface where the fluid is non-Newtonian, there are plenty of precipitate wax particles but, in real systems, asphaltenes are present. The problem is that the only literature regarding the influence on rheological behavior on diffusion coefficient is with polymers. This is a hot topic in several industries, but it is impossible to extrapolate to rheological behavior of waxy crude oil because the polymer's molecular weight is up to three orders of magnitude higher than that of asphaltenes [91].

To highlight the necessity of improving the measurements of molecular diffusion coefficient. Using Van Der Geest et al. [14], viscosity *vs.* temperature curve, shown in Figure 7, when below $T = 26\ °C$, the oil has a shear thinning behavior. At the wall, the shear rate is the highest and the temperature is the lowest. As the distance from the interface increases, if the viscosity decrease (due to higher temperature) is smaller than the viscosity increase (due to shear rate decrease), the molecular diffusion coefficient could reach a minimum point that is not at the wall, thus a decrease in mass flux compared to classic models. This could be the mechanism behind the speculations in shear reduction, as shown in Figure 7. There is no evidence that this occurs, since it is based on the correlation from Hayduk and Minhas [30], which seems to be inaccurate for complex non-Newtonian Mixtures.

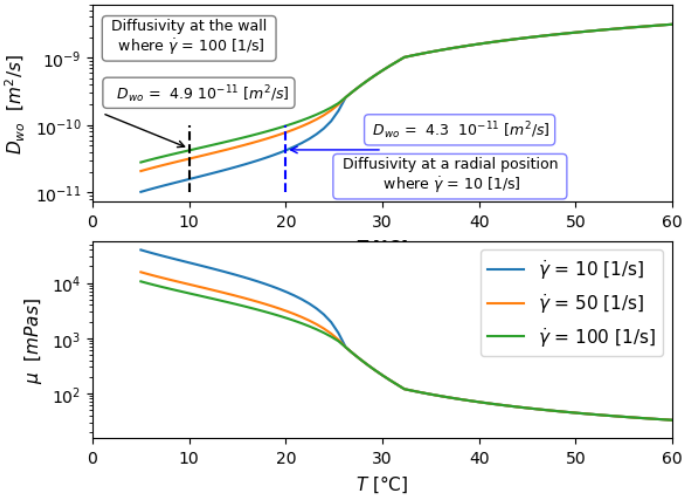

Figure 7: Viscosity vs Temperature for Brazilian waxy crude oil [14]. Calculation of Molecular diffusion coefficient using Hayduk and Minhas

There is another way of seeing how strongly the rheology can influence the molecular diffusion coefficient, which is considering the concept of yield stress. Assuming the fluid behaves as Herschel Bulkley [24][26] or Bigham [47] [86], and using Hayduk and Minhas' equation, the diffusion coefficient tends to zero where plug flow occurs because the viscosity goes to infinity. The main point is that the error involved in applying those correlations to non-Newtonian behavior is unknown. It is most likely inaccurate, but that needs to be experimentally verified and the errors quantified.

Zheng et al. [26] solved momentum conservation, heat and mass transfer for turbulent flow considering a Non-Newtonian viscoplastic fluid. To facilitate the convergence of numerical solutions, the authors applied the concept of apparent yield stress where, for low shear rates, the viscosity is massive, but finite, and thus used a modified Herschel-Bulkley model. They demonstrated that applying LES (large eddy simulation) and RANS (Reynolds-averaged Navier–Stokes) simulation to solve radial mass / heat transfer equation results in drastically different temperature and concentration profiles because RANS fails to accurately predict turbulent diffusivities. They concluded that, for non-Newtonian cases, the use of RANS underestimates the heat and mass transfer and thus cannot be used to model wax deposition for turbulent flow.

To our knowledge, not a single study was able to experimentally test or isolate the effects of non-Newtonian behavior in wax deposition. That is a complex task because there are several other phenomena occurring simultaneously, thus it not easy to isolate the influence of the constitutive equation in the concentration gradient kinetics or on the characteristics of the deposit.

Wang et al. [74] used the concept of non-Newtonian viscoplastic fluids to a modified shear dispersion equation, more specifically using a power-law constitutive equation. They adjusted several empirical variables to the cold finger data and assumed that the shear dispersion term would be equal in both the pipeline and the cold finger. This kind of analogy poses the same problem as the classic shear stripping fitting [31][38], where one can fit experimental data, but cannot actually model the phenomenon of fracture and removal of wax from the deposit.

$$\dot{m}_{bd} = A_i D_{sd} \left(\frac{\tau}{K} \right)^{\frac{1}{n}} \tag{26}$$

Todi [92] shows the variation of the velocity and stress profiles for non-Newtonian power law fluids. Interesting results of the error between measurement, using PIV, and modeling of such profiles are shown. One argument is that the stress profile is independent of the heat flux condition for power-law fluids: heating, cooling, and zero heat flux, for the presented experimental matrix. This is unexpected for highly non-Newtonian fluids, since the viscosity can change dramatically with temperature

6. Deposit

When studying the deposit, the two big questions are how the deposit grows and ages over time. Aging is the increase of the average weight fraction of the deposit and growth is the change in the thickness of the deposit. There are three main approaches to model aging, the most common in the literature is the counter molecular diffusion [13], there is also the Ostwald ripening [15] and shear deformation of a cubical cage [18]. All hypotheses regarding the aging phenomena directly influence the calculation of the thickness of the deposit, which are related to the mechanisms discussed in the previous sections.

To highlight what shall be discussed in the following sections, all models contain hypotheses regarding the morphology of the crystals inside the deposit and there is a lack of experimental data on the morphology and crystalline structure; *i.e.*, the porous structure of the deposit. It is not trivial to measure the microscopic behavior of the deposit in a wax deposition experiment. For this reason, the models were not validated experimentally and the phenomenon is not well understood.

It is accurate to assume that the entire mass of wax within the deposit, at any given time, is the multiplication of the deposit mass vs the wax weight fraction [3]([10]. Thus, the time derivative is

$$\dot{m} = \frac{d}{dt} \left[\pi L \rho_{dep} \left(R^2 - r_i^2 \right) \bar{F}_{w_{dep}} \right] \tag{27}$$

From mass transfer-based models, it is understood that wax molecules transferred to the deposit cause two consequences. First, they can increase the weight fraction of wax in the deposit (aging). Second, wax thickness can increase (growth). Then, assuming that the deposit initially has a constant density and thickness in the L length, from Equation 27 it is possible to obtain:

$$\dot{m} = \overbrace{\pi L \rho_{dep} \left(R^2 - r_i^2 \right) \frac{dF_{w,dep}}{dt}}^{\dot{m}_{Aging}} - \overbrace{2\pi r_i L \rho_{dep} F_{w,dep} \frac{d\left(r_i\right)}{dt}}^{\dot{m}_{Growth}} \tag{28}$$

6.1. Aging by Counter Molecular Diffusion

It is important to highlight that, in Equation 28, there is no assumption regarding any mechanism. This is the point where the discussion begins on the hypothesis and mechanisms involved in modeling the deposit. Most simulators use some variation of the model proposed by Singh et al. [3] for the deposit, which considers the deposit at thermodynamic

equilibrium. The mass transferred from the interface into the deposit is equal to the aging term of Equation 28.

$$\dot{m}_{Aging} = A_i \left(-D_{eff} \frac{\partial C_i}{\partial r} \right) \tag{29}$$

$$\overbrace{\pi L \rho_{dep} \left(R^2 - r_i^2 \right) \frac{\partial F_{w,dep}}{\partial t}}^{\dot{m}_{Aging}} = 2\pi r_i L \left(-D_{eff} \overbrace{\frac{\partial C}{\partial T}\bigg|_{T_i} \frac{\partial T}{\partial r}\bigg|_{r_i}^{+}}^{equilibrium} \right) \tag{30}$$

By solving the equations discussed in the last section for the bulk, it is possible to obtain the total mass transferred to the deposit at any given time. Equation 30 is used to calculate the aging and, from Equation 28, it is possible to obtain the mass that increases the deposit's thickness. The counter molecular diffusion model, as proposed by Singh et al. [3], does not consider molecular kinetics and crystallization as a factor that directly influences the thickness of the deposit. This fact is important because, when modeling the deposit in diffusion-based models, the only way to account for the influence of wax crystal size and morphology in the thickness is through the following process:

Molecular size increase $\longrightarrow$ Aspect Ratio increases $\longrightarrow$ Diffusivity of the deposit decrease $\longrightarrow$ Aging decrease $\longrightarrow$ Growth increase

This method assumes that all variation in the crystalline structure is either parallel to the interface or the growth is toward the wall. Thus, the crystal growth cannot increase the size of the deposit directly, which seems problematic since crystallization at the interface during wax deposition is certainly an important part of the phenomena. Thus, for a more accurate modeling, important aspects of crystallization in the interface should be understood.

6.1.1. Diffusion Coefficient

For the discussion of the deposit by counter molecular diffusion, one of the most important aspects is quantifying the wax diffusivity coefficient in the deposit - the effective diffusivity (D_{eff}). Singh et al. [3] proposed using the model derived by Cussler et al. [93], which assumes that diffusion occurs on the slits between bricks (wax crystals). A schematic is shown in Figure 8, similar to what was proposed by Cussler et al. [93].

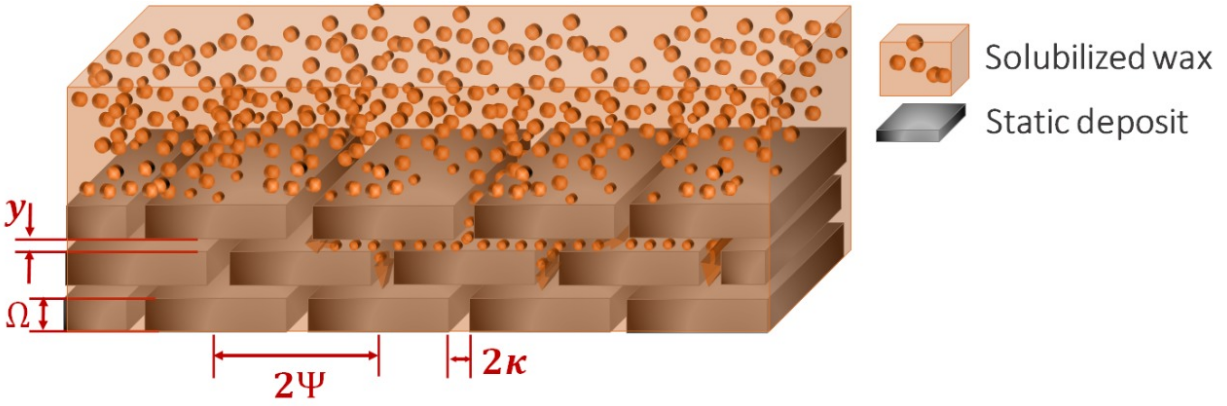

Figure 8: Schematic of the deposit configuration [39] [93]

Cussler et al. [93] started by defining the geometrical and morphological parameters involved in the model, the aspect ratio of the bricks, from now on called aspect ratio of wax crystal (α), the aspect ratio of the slits (Γ) and the

volume fraction of the deposit (Φ).

$$\alpha = \frac{\Psi}{\Omega}; \Gamma = \frac{\kappa}{\Omega}; \Phi = \frac{\Omega}{\Omega + y} \tag{31}$$

At this point, they consider the density of the deposit constant. Thus, the average volume fraction becomes the average weight fraction ($\phi \sim \bar{F}_{w,dep}$). With the definition shown in Equation 31, Cussler et al. [93] derived:

$$D_{eff} = \frac{D_{wo}}{1 + \Gamma\alpha\bar{F}_{w,dep} + \frac{\alpha^2\bar{F}^2_{w,dep}}{(1-\bar{F}_{w,dep})}} \tag{32}$$

Considering the same geometrical definitions, Aris [94] derived a similar equation [13]:

$$D_{eff} = \frac{D_{wo}}{1 + \frac{\alpha\bar{F}_{w,dep}}{\sigma} + \frac{\alpha^2\bar{F}^2_{w,dep}}{(1-\bar{F}_{w,dep})} + \frac{4\alpha\bar{F}_{w,dep}}{\pi(1-\bar{F}_{w,dep})} \ln\left[\frac{\pi\alpha^2\bar{F}_{w,dep}}{\Gamma(1-\bar{F}_{w,dep})}\right]} \tag{33}$$

Then, Singh et al. [3] applied the assumption that the pore aspect ratio is much smaller than the wax crystal aspect ratio ($\Gamma << \alpha$), which leads to the equation used by all software, based on the model from Singh et al. [3]:

$$D_{eff} = \frac{D_{wo}}{1 + \frac{\alpha^2\bar{F}^2_{w,dep}}{(1-\bar{F}_{w,dep})}} \tag{34}$$

Figure 9 shows the general behavior of the effective diffusivity for the deposit. It is interesting to observe that, as the aging process occurs, *i.e.*, an increase in the average molecular weight of the deposit, the effective diffusivity decreases. This was expected due to the decrease in the porous aspect ratio (σ). All results shown in Figure 9 consider the same molecular diffusivity of wax on oil (D_{wo}).

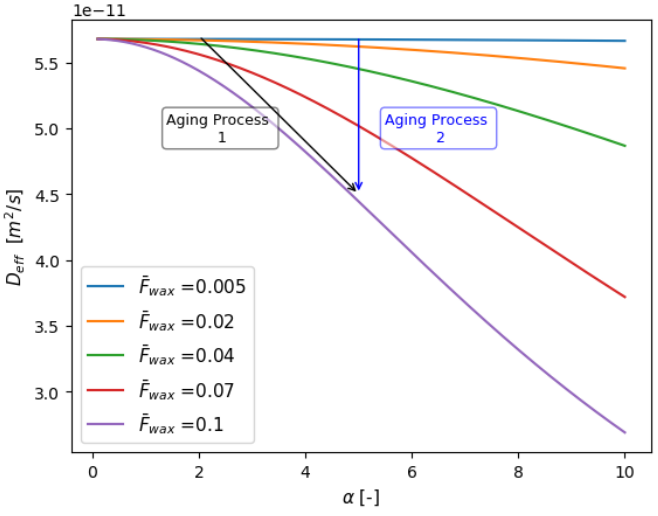

Figure 9: Effective Diffusivity of the deposit vs aspect ratio for different average molecular weight fraction

The literature commonly uses the wax aspect ratio (α) to fit the data. Singh et al. [3], for example, assume a linear

relationship between the average molecular weight and the wax aspect ratio [95], as shown in Equation 35. That is a strong assumption and has no experimental background to support it under flow condition, as shown by Soedarmo et al. [95]. The variation of the aspect ratio can lead to drastic variations in the predictions of the deposit's thickness and composition [96]. Soedarmo et al. [23] used a value of $a_\alpha = 5$ for comparing experimental data and simulation results.

$$\alpha = 1 + a_\alpha \bar{F}_{w,dep} \tag{35}$$

If the deposit already starts with the $\sigma << \alpha$ hypothesis being correct, and that counter molecular diffusion is the only aging mechanism for the deposit, there is still a question to answer: how does the aging process evolve? In Figure 9, two possible ways of aging are illustrated. In the first (aging process 1 – Figure 9), there is an increase in both the average molecular weight of the deposit and an increase in the aspect ratio, which is similar to what [3] proposed, and was used by [23]. In the second (aging process 2 – Figure 9), there is an increase in the average molecular weight of the deposit, but the aspect ratio of the molecules does not increase and more molecules are therefore present in the deposit - smaller molecules. The only experimental evidence points to the aging process 2 for laminar flow [95].

The aspect ratio ranges between 2 and 3 according to the only experimental research, known by our group, which has investigated the aspect ratio under flow conditions for laminar flow [39]. If that was the case for every crude and flow condition, including turbulent flow, then the effective diffusivity would not vary much. This assumption needs to be verified, mainly regarding the turbulent flow for which we have no experimental evidence on the aspect ratio. One way of doing so is by experimental research linking a microscope to a flowloop and performing tests at different flow conditions.

6.2. Aging by Ostwald Ripening

Coutinho et al. [97] took a different approach and showed that there is a second mechanism involved in aging, based on re-crystallization, called Ostwald Ripening [98]. Their research showed that, even under isothermal conditions, where molecular diffusion stops, there is molecular growth in the deposit and thus, aging.

6.3. Aging by Shear Deformation of a Cubical Cage

Differently than Coutinho et al. [97], who showed a secondary mechanism for aging under isothermal conditions, Mehrotra et al. [6] proposed a completely different approach for modeling the increase in average molecular weight of the deposit with time and shear stress.

The cubical cage model [18] [99] [85] [6] represents the wax deposit layer under static conditions as a lattice-like structure, where each unit cell is a cubical cage with side Υ and volume V, its deformation is used to predict the wax deposit aging. It is a simple approach that does not intend to predict the configuration of solid and liquid phases, but only determine how the deposit composition changes over time and shear stress. It only depends on the determination of two parameters (Z and β). The volume fraction of each phase is related to the ratio (Z) of the cubical cage edge thickness (ξ) to the cubical cage side (Υ). This ratio (Z=ξ/Υ) is fixed for static conditions and can be determined from liquid-solid phase equilibrium calculations. Equation 36 provides the volume fraction of the solid phase, which is represented by the edges of the cubical cage. Equation 37 provides the volume fraction of the liquid phase, which is the remaining part of the cubical cage (total volume minus the volume of the edges).

$$V_S = (12Z^2 - 16Z^3) \tag{36}$$

$$V_L = (1 - 12Z^2 - 16Z^3) \tag{37}$$

If a one-dimensional shear stress is applied in the direction of the flow, the cubical cage will deform by tilting in the same direction at an angle β and release liquid (solid phase is preserved). This angle is correlated with the shear stress (or Reynolds number) and deposition time [99]. Consequently, the volume fraction of each phase (solid and liquid) after deformation (indicated by the index β) is obtained by dividing the volume of the static cage by $\cos\beta$. The overall change in the volume will give the volume of liquid released from the cubical cage (Equation 38), which can

be related to the changes in the average weight fraction of the deposit: *i.e.*, aging [85].

$$V_{cage} - V_{cage\beta} = V_L V_{cage} - V_{L\beta} V_{cage\beta} = (1 - cos\beta)a^3 \tag{38}$$

The results show that β increases with the shear stress (or Reynolds number), but no mathematical relationship between these variables is available [99]. At the maximum angle ($\beta_{max} = cos^{-1}(12Z^2 - 16Z^3)$), the liquid phase is completely released from the cubical cage. Thus, the higher the β, the higher the concentration of wax and the heavier the n-alkanes will be in the deposit. This increase of the deposit weight fraction corresponds to the deposit hardening and causes an increase in the deposit's thermal conductivity. Finally, the change in the thermal conductivity will impact the heat transfer calculations that govern the deposit's growth [6].

Mehrotra et al. [6] show results where experimental data properly match predicted data and, using the cubical cage model, explain the faster time scale of aging observed experimentally for turbulent flow. Aging by cubical cage deformation is a more simplistic approach and presents a good agreement with experimental data. However, the methodology used to develop its mathematical model must still be better explained and validated with a broader database. This fact does not justify neglecting it or assuming the counter molecular diffusion model as the only correct mechanism. Both models can be scrutinized and future researches need to expose and compare them in order to conclude which is the best, or even to develop a better model. The only way to better model the aging phenomenon is through a deeper study of how the crystal morphology and the porosity of the deposit vary over time.

7. Boundary: Interface

There is little discussion on what happens at the bulk-deposit interface. However, a number of open questions and mechanisms might be relevant. The first focus is on the mass that reached the interface and the second on the precipitated wax in the vicinity of the interface. There is an interesting discussion in Ravichandran [49] about the possibility of the interface not being in equilibrium, but in a supersaturated state. This would suggest that the calculation for the concentration gradient is wrong in most models.

The second open question is based on visualization studies that show an axial movement of wax particles at the interface until they decelerate and stop, becoming part of the deposit. The first study was below WAT [28] and showed that the thickness of the deposit can double with suspended crystals. In the second study, the bulk was above WAT, but there were crystals in the mass transfer boundary layer [49]. In both studies, it was possible to observe the axial displacement of crystals in the vicinity of the interface, then stopping and becoming part of the deposit. To our knowledge, this phenomenon is disregarded in every simulator.

The work of [28] presents an interesting video by a camera installed in the experimental apparatus. The video shows the interface of the deposit and the behavior of the wax crystals in the vicinity of the interface. This result corroborates with the necessity of further investigation on the interface to better represent the effects of new particles on the entire deposit. The authors found differences in deposit thickness formed under the presence of suspended flowing wax crystals, indicating the importance of crystals suspended in solutions flowing with temperatures below the WAT. It was observed that wax crystals and agglomerates present trajectories nearly parallel to the channel wall. These crystals and agglomerates were seen to decelerate and stop, being incorporated into a thin wax deposit formed in the initial cooling stages.

On the other hand, several studies under cold flow conditions show no increase in the deposit compared to hot flow regimes [85, 100], thus, precipitated wax would not cause any increase in the thickness of the deposit. There is a clear discrepancy between carefully executed experiments, which may be related to the size of the particles in the vicinity, individual wax crystals do not deposit, but an agglomeration of the wax crystal can reach a critical size that would deposit, another hypothesis that needs to be tested.

Figure 10 shows a schematic of the effects described above. The wax crystals reach the interface but do not become part of the deposit and flow near the boundary until they stop and increase the deposit's thickness.

The adhesion of the wax particle to the wall depends on the material of the pipeline. Coating the pipe with wax repellent surface, such as glass or polymers, has proven to reduce wax deposition [35] [29] [101] [102]. The work of Jessen and Howell [35] was one of the first to investigate this. The authors studied the wax deposition in different pipe materials (plastic, aluminum, and steel) under different conditions of hardening, shear, and cooling rates.

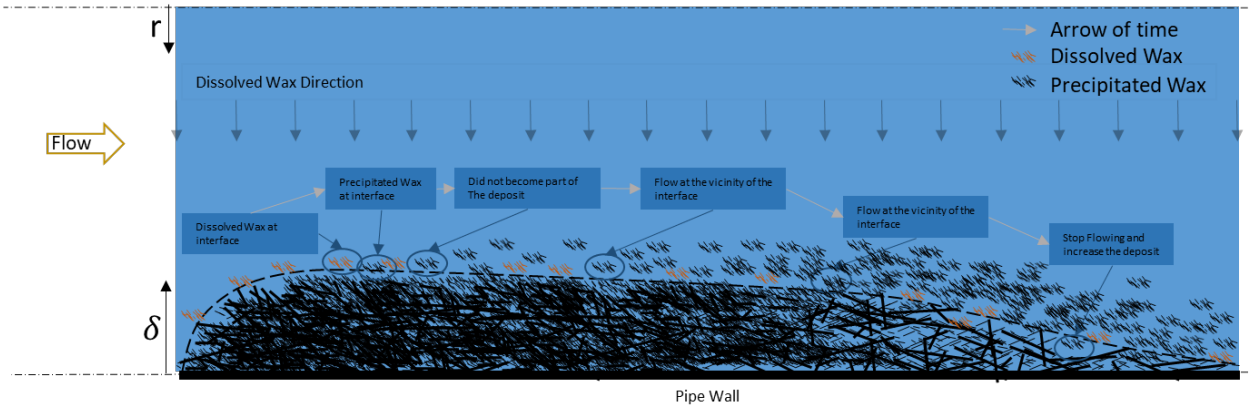

Figure 10: Schematic of the possible interface containing the effect of crystal dragging and deposition in posterior regions further along the deposit

8. Start of wax deposit

Another topic to discuss is how the deposition starts, and there are few studies on the beginning of the wax deposition. To understand the beginning, it is necessary to understand the beginning of the wax precipitation itself. As stated before, wax precipitation is analog to any crystallization process. Consequently, all the assumptions valid for a crystallization process must be valid for wax precipitation:

1. Exothermic process
2. Nucleation is a stochastic event
3. Crystal will only precipitate at favorable temperature and pressure conditions.

Wax precipitation will release temperature (exothermic process), so the preferable place for wax precipitation is where the system can better absorb the released temperature. As a consequence, (a) there will be a preferable place for wax precipitation in the system studied, and (b) this preferable place will begin generating a concentration gradient. Two possible mechanisms have been considered for starting the wax deposition[26, 49]. It is important to highlight that the mechanism discussed below can occur simultaneously; there is no evidence that it must be one or another.

8.1. Rheological Problem

To understand how a deposit would start assuming the rheological perspective, the definition of yield stress should be presented. Basically, there is a threshold below which the applied stress would not cause a shear and the fluid would strain, but not flow. Just for scientific clarification, there is a debate whether this definition is appropriate, but it shall be presented here as Bingham did, since only the engineering aspect of the yield stress concept will be explored, instead of the predictability in infinite time scales.

$$\sigma = \sigma_0 + \mu\dot{\gamma} \tag{39}$$

In Figure 11 shows the hypothesis that the deposit starts due to the increase in the viscosity up to infinity, which is another way to see the yield stress. In x_0, there is no deposit and the fluid behaves as a Newtonian fluid. If we assume turbulent flow, in the boundary layer, we have the classic description of inner layer and outer layer. This discussion, however, is outside the scope of this review. For clarity, the system is divided into three regions: the viscous laminar sublayer, the overlap layer, and the turbulent outer layer [103].

At axial point x_1, there is no static deposit and the dark grey area corresponds to non-Newtonian behavior. As the wax crystals precipitate and the apparent viscosity increases significantly, the oil behaves as non-Newtonian, thus the velocity profile approaches the velocity profile of a shear thickening fluid under isothermal flow conditions. This means that the velocity and, thus, the shear rate decreases significantly. As more and more particles precipitate, at some point, the fluid starts to present yield stress. Another way to describe this is considering that the viscosity in the

laminar sublayer increases so drastically that the sublayer is divided into two, one with the Newtonian flow and the other with the non-Newtonian flow.

As more wax particles precipitate, the yield stress of the fluid increases, this has been observed in numerous bench experiments [25]. Once the yield stress of the fluid overcomes the stress at the wall, the flow in the laminar sublayer stops and the deposit thus begins [26].

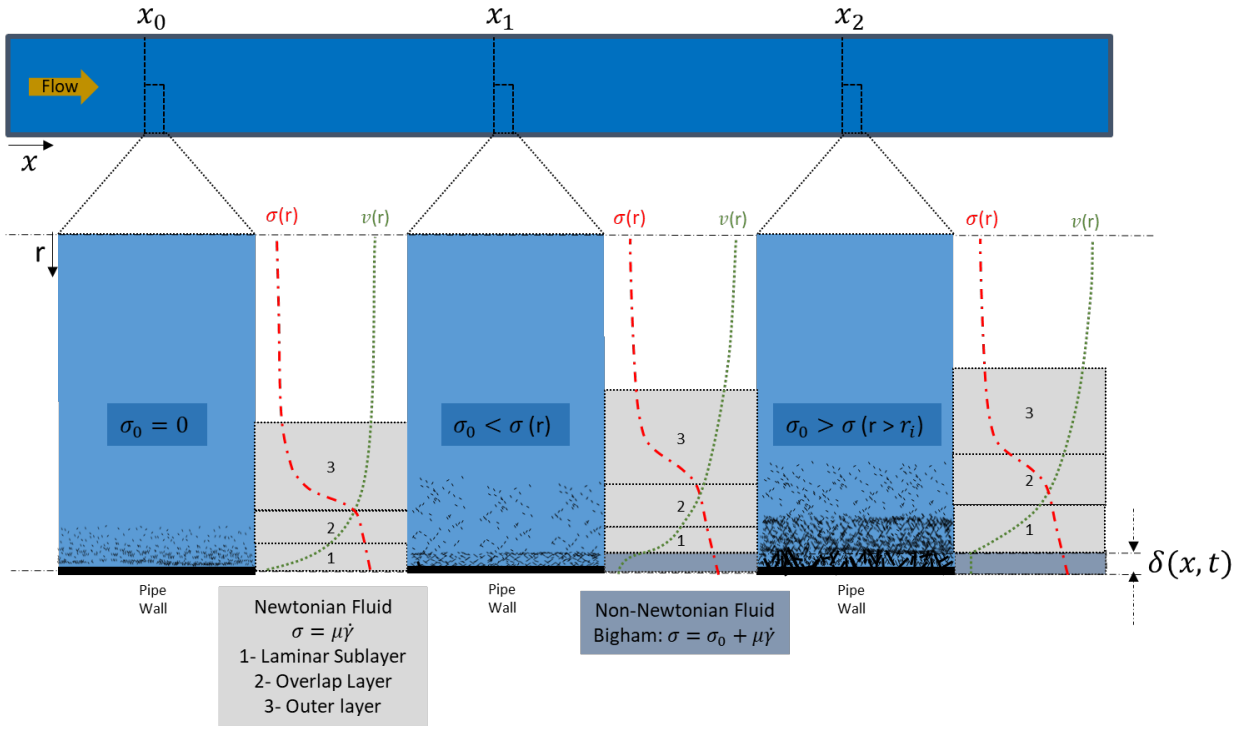

Figure 11: Schematic of deposition starting based on yield stress definition

8.2. Phase Change Thermodynamic problem

This is classic nucleation theory [104]. Since the temperature at the wall is lower than the WAT, some nuclei of wax particles start to precipitate, but they are not big enough to be stable. Once they reach a limit size, named critical nucleus size, they become stable and other particles attach to the newly-formed nuclei and the crystal grows. Every nucleus smaller than the critical size dissolves again into the bulk [13].

Figure 12 shows a schematic of this process in three phases: at the first axial point x_0, there is a radial point where the temperature is lower than the WAT, at that point small wax crystals start to precipitate, dissolved wax molecules are represented in orange and the precipitated crystals in black. As time and the position evolve due to flow, the crystals keep randomly precipitating and solubilizing in a stochastic process. At some point, shown in x_1, some crystals reach the Gibbs free energy necessary that a nuclei size is big enough to be stable. From this point forward, smaller crystals attach to the formed stable crystal, increasing its size. When enough of these stable crystals are formed at the wall, the deposit will start to grow, both by increasing the size of the crystals and by new crystals being formed.

To quantify the critical nuclei size, it is necessary to overcome the classic Gibbs Free energy change of precipitation, which is maximum at the critical nucleus size concerning the number of wax molecules (N), thus the derivative is zero. In classic crystallization publications, the critical size is related to the radius (critical radius) but, for the discussion in terms of the population balance, it is better to use the number of wax molecules.

$$\frac{\partial\left(\frac{\Delta E_{Gibbs}}{kT}\right)}{\partial N} = 0 = \frac{2}{3} g^{-\frac{1}{3}}\,\theta - \ln S_s \tag{40}$$

$\theta = \frac{\sigma_f S_1}{KT}$, σ_f is the surface tension between wax and oil (dyne/cm), S_s is the degree of supersaturation, as discussed in [49], S_1 is the surface of wax molecule (cm^2).

In Figure 12, the interface is not at WAT, because that has not proven to be the case. For simple fluids, the crystallization would occur at a constant temperature, but the representation is of a complex mixture, which can present supersaturation effects where the equilibrium has not been reached.

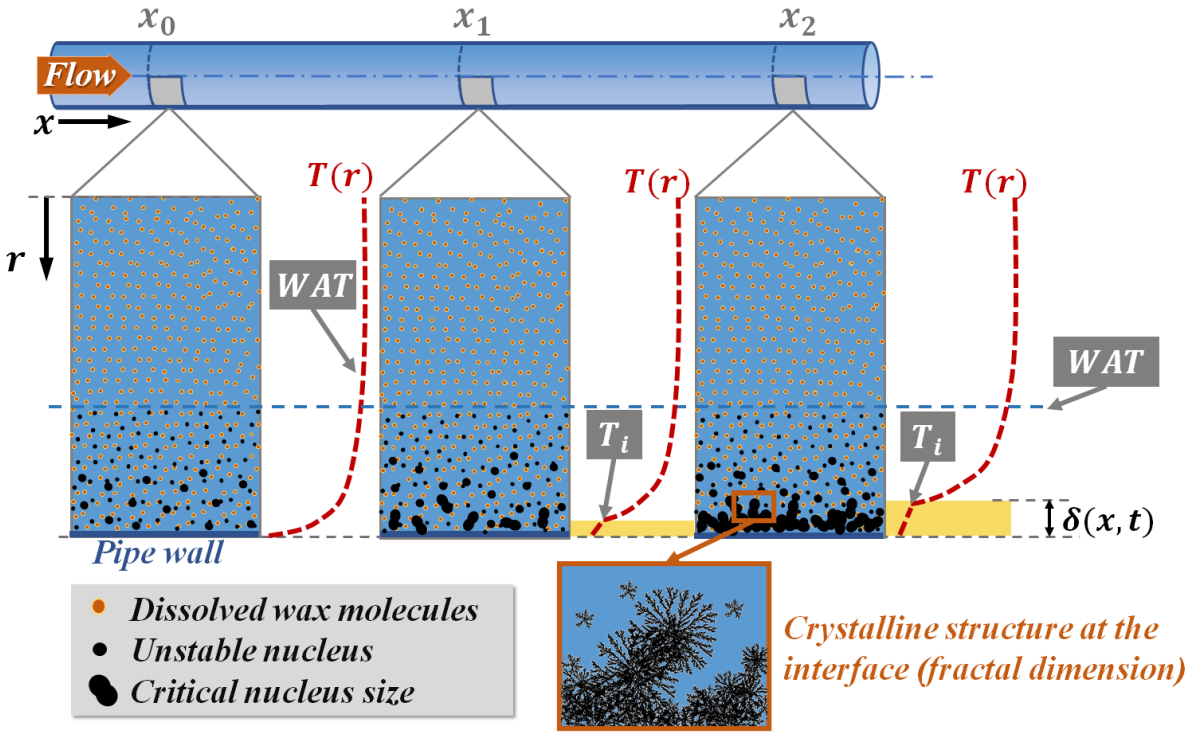

Figure 12: Representation of deposit start-up based on critical nucleus size

9. Wax Deposition Simulators

Wax deposition simulators, commercial and academic, are mainly based on mass transfer models.

9.1. Commercial

Commercial multiphase flow simulators, such as OLGA (Schlumberger), LedaFlow (Kongsberg) and ALFAsim (ESSS), are widely used in the Oil Gas industry. The wax module in OLGA (OLGA Wax) calculates deposition and wax transport through one of three models: RRR, Heat Analogy, and Matzain diffusion model [81]. The wax module in LedaFlow can simulate the wax formation and melting to determine the pigging frequency to keep wax under control [105]. The module is based on the work shown in [13] and [92]. It models wax crystallization; *i.e.*, wax precipitation in the bulk forming a slurry and wax deposition caused by radial diffusion of wax molecules [82]. A sensitivity study was performed by [82] comparing results obtained from OLGA and LedaFlow. The effect of adjustable parameters for the wax deposition in both software was evaluated and both presented problems in reproducing the pressure behavior.

The wax module in ALFAsim enables calculating the wax deposition rate using the Matzain diffusion model, and also its influence on pressure drop and heat transfer, thus predicting the risk of plugging by wax [106]. ALFAsim is the most recent flow simulator developed, and not much information was found about it in the open literature.

9.1.1. RRR model

The RRR (Rygg, Rydahl and Rønningsen) model is limited for turbulent flow. In this model, the predicted amount of wax deposited is obtained considering molecular diffusion and shear dispersion. There is no consideration of wax

removed by shear effect, but it considers the wax dissolution [107].

9.1.2. Heat Analogy

The Heat Analogy comes from the Film Mass and Transfer (FMT) model based on molecular diffusion and explained in section 4.1.2.2. It includes the effects of shear dispersion and shear removal (stripping).

9.1.3. Matzain model

The Matzain model, introduced in section 4.2, is a semi-empirical model based on molecular diffusion and accounts for shear dispersion (low importance) and shear removal, by adding two empirical parameters to Fick´s Law. For turbulent flow, the Matzain model is equivalent to the Heat Analogy [107]

9.2. Academic

There are two well-known wax deposition simulators developed by academia. The first, called TUWAX, was developed by a research group at The University of Tulsa working on the Paraffin Deposition Project. It is based on the mass transfer models for wax deposition and is mainly validated through their in-house loops experimental data [108]. As per their website [109], the model is valid for single and multiphase mixtures, and is constantly updated by the group.

The second is called Michigan Wax Predictor (MWP) developed by the University of Michigan's Porous Media Research Group [108] [110]. This simulator was the first to account for aging following the work of [3] and, since then, the simulator has been constantly updated. The simulator is validated by experimental data from loops around the world [111]. The Michigan Wax Predictor is a software package available from the University of Michigan's Industrial Affiliates Program [111]. As the other software, it considers the classic effects: molecular diffusion, shear rate reduction and sloughing. However, in a recent thesis [112], they have presented a model coupling transient mass transfer and transient heat transfer. The first, mass transfer, is the classic wax deposition modeling. The last, heat transfer, corresponds to what we introduced as phase transition, which they named gelation, claiming it only occurs because the waxy oil mixture achieves a yield stress and forms a gel-like structure. They defend that both mechanisms have to be taken into account when modeling wax deposition, regardless of which one is controlling the process. To our knowledge, this is the first software to consider the phase transition mechanism.

10. Conclusion

Wax deposition in pipelines is a complex phenomenon that has been discussed thoroughly both in Academia and Industry for several decades. This paper is a critical review of the most important aspects of the opinion of the authors. We separated the paper into sections to increase clarity for the reader, the paper was divided into a general view: state of the art, then a section for energy conservation, followed by the mechanism for Newtonian fluid, then mechanisms for non-Newtonian fluid, a discussion of the deposit, both aging and growth effects, and then the interface. Finally, a brief discussion on the beginning of wax deposition and the available simulators.

For at least the last decades, most of the community has converged to the conclusion that molecular diffusion is the controlling mechanism for wax deposition. As has happened in the past for shear-related phenomena, the growing experimental evidence shows that molecular diffusion is insufficient and several research groups are looking for an explanation of the discrepancy between model and data.

In the literature of mass transfer-based mechanism, the most common way to explain the discrepancy is by applying shear related phenomena, the shear stripping (sloughing) is the most common mechanism in the last decade. The argument is that, as the Reynolds number increases, so does the stress at the interface, which removes parts of the solid deposit. This is an indirect conclusion without concrete experimental evidence, based on the fact that, as the Reynolds number increases, the thickness of the deposit is smaller. It is important to highlight this because there is another explanation, often overlooked by the literature of mass transfer-based wax deposition, given by phase transition based models.

There is a viable experiment that is necessary to verify which is the correct approach to model wax deposition - the measurement of the interface temperature. Although there are many flowloops throughout the world, there is limited data of the interface temperature, all the experimental evidence points to a constant interface temperature. This is very relevant because, if the temperature of the interface is constant throughout the deposition process, this indicates a phase transition phenomena. In parallel, it would also mean no increase of the thickness according to existing mass transfer models. Therefore, the most accepted models applied by all commercial simulators would be wrong.

This review has shown that the most important parameter of molecular diffusion predictions, the diffusion coefficient of wax in oil, is still not well determined. The widely-used correlation of Hayduk and Minhas (all commercial and academic simulator) produces doubtful results when compared to real data; the correlation was obtained from data with molecules with up to C32. A new experimental study with more complex mixtures must be performed and new correlations, based on physics (dimensionally correct), are necessary to improve prediction of mass transfer-based models.

The non-Newtonian influence on wax deposition is more recently being addressed. It is important to highlight that, when it comes to fluids with non-Newtonian behavior, the classic correlations widely used to obtain the dimensionless parameters (Nu, Pr, Sh, Sm) have not been verified and are probably wrong. The influence of the non-Newtonian fluid on mass and heat transfer properties need to be better investigated, but a challenge that needs to be overcome is how to isolate and study this subject experimentally.

An important point lacking experimental study, due to its complexity, is the microscopic behavior of the crystals and pores of the wax deposit under flow. Despite the approaches to modeling the deposit, this investigation is important to assess if the molecular kinetics (growth) and wax crystal morphology are factors influencing the thickness of the deposit. The assumptions regarding the geometrical distribution and porosity of the deposit are poorly verified, but they are still very common in all simulators.

The only experimental evidence under flow conditions indicates aspect ratio ranging between 2 and 3 for laminar flow, if this is true for every crude and flow condition, it implies that the effective diffusivity would not vary much. This assumption needs to be verified, mainly regarding turbulent flow, for which no experimental evidence on the aspect ratio was found. The lack of data on the aspect ratio of wax crystals in the deposit is common in mass transfer-based models as a fitting-tool to "correct" the predictions of such models.

Finally, there is the behavior of precipitated wax crystals at the bulk in the vicinity of the interface. Most studies show that precipitated crystals in the bulk of the vicinity of the interface do not necessarily increase the thickness of the deposit, but a number of recent studies have measured the increase of the deposit in such conditions.

11. Acknowledgments

The authors wish to thank EQUINOR for their financial and technical support in this study. We also thank ANP (National Agency of Petroleum, Natural Gas and Biofuels). We thank the School of Mechanical Engineering (FEM) and the Center for Petroleum Studies (CEPETRO) at the University of Campinas (UNICAMP). Acknowledgments are also extended to ALFA research group for their support.

Nomenclature

Physical Properties

α	Crystal aspect ratio $[-]$
$\dot{\gamma}$	Oil shear rate at pipe wall $[1/s]$
Γ	Slits aspect ratio $[-]$
γ	Exponent of Hayduk-Minhas correlation $[mol/m^3]$
κ	Cubic cage edge thickness $[m]$
μ	Viscosity $[Pa.s]$
Ω	Deposit slit thickness $[m]$
Φ	Volume fraction of the deposit $[-]$
Ψ	Half slit size $[m]$
ρ	Density $[kg/m^3]$

τ	Stress $[Pa]$
Υ	Cubical cage edge size $[m]$
ξ	Cubical cage edge thickness $[m]$
A	Area $[m^2]$
C	Concentration $[kg/m^3]$
c_p	Specific heat coefficient $[m]$
D	Diffusivity $[m2/s]$
E	Elastic modulus $[Pa]$
E_{Gibbs}	Gibbs free energy $[J]$
G	Intrinsic fracture Energy $[J]$
Gz	Graetz number $[-]$
H	Latent heat $[J/kg]$
k	Thermal conductivity $[W/mK]$
k_M	Mass transfer coefficient $[m/s]$
M	Molar mass $[kg/mol]$
M	Molecular weight $[kg/mol]$
m	Mass, $[kg]$
N	Number of wax molecules $[-]$
Nu	Nusselt number $[-]$
p	Pressure $[Pa]$
Pr	Prandtl number $[-]$
q	Heat $[J]$
R	Pipeline radius $[m]$
r	Radial direction $[m]$
Re	Reynolds number $[-]$
S_s	Supersaturation ratio $[-]$
Sh	Sherwood number $[-]$
T	Temperature $[°C]$
t	Time $[s]$
U	Internal Energy $[J]$
u	Velocity $[m/s]$
V	Cubical cage volume $[m^3/mol]$

x Axial direction $[m]$

y Distance between deposit slits $[m]$

Z Ratio of the cubical cage edge thickness (ξ) to the cubical cage side (Υ) $[-]$

Constants

φ Wilke-Chang association parameter, $[-]$

Subscripts

a Aggregated wax crystals

$Aging$ Aging process properties

$b/bulk$ Bulk properties

bd Brownian diffusion properties

$cage$ Cubic cage properties

$cage\beta$ Properties of cubic cage deformed by tilting at β angle

$coolant$ Coolant properties

dep Deposit properties

eff Effective property

eq Equilibrium condition properties

$Growth$ Growth process properties

i Interface

in Inner radius

L Liquid

md Molecular diffusion

n Non-aggregated wax crystals

o Outer radius

p conductivity at constant pressure

pp Pour Point

r Radial

S Solid

sd Shear dispersion properties

w Wax properties

$wall$ Property of the pipe wall

wo Wax in oil properties

x Axial

Abbreviations

WDT	Wax dissolution temperature
DSC	Differential Scanning Calorimetry
EM	Equilibrium model
FMT	Film Mass Transfer
LES	Large eddy simulations
OG	Oil and Gas
$RANS$	Reynolds averaged Navier–Stokes
WAT	Wax appearance temperature

Mathematical Operator

$:$	Double Inner Dot Product
$\bar{}$	Average
$\cdot$	Inner Dot Product
Δ	Delta
∇	Nabla operator
∂	Partial derivative
$\vec{}$	Vector
d	Full derivative

Empirical parameters

a	empirical parameter
b	empirical parameter

Subscripts Authors

Bur	Burger et al. [34]
Cor	Correra et al. [33]
Fas	Fasano et al. [47]
Mat	Matzain [31]
Mer	Merino-Garcia et al. [1]
Ram	Ramirez-Jaramillo et al. [72]

CRediT authorship contribution statement

Charlie van der Geest: Conceptualization, Methodology, Writing - Original draft preparation. **Aline Melchuna:** Methodology, Writing - Original draft preparation. **Letícia Bizarre:** Writing - Original draft preparation. **Antonio C. Bannwart:** Supervision. **Vanessa C. B. Guersoni:** Conceptualization, Review, Supervision.

References

[1] D. Merino-Garcia, M. Margarone, and S. Correra, "Kinetics of waxy gel formation from batch experiments," *Energy and Fuels*, vol. 21, no. 3, pp. 1287–1295, 2007.

[2] M. C. K. De Oliveira, R. M. Carvalho, A. B. Carvalho, B. C. Couto, F. R. Faria, and R. L. Cardoso, "Waxy crude oil emulsion gel: Impact on flow assurance," *Energy and Fuels*, vol. 24, no. 4, pp. 2287–2293, 2010.

[3] P. Singh, R. Venkatesan, and H. S. Fogler, "<Formation and Aging of waxes 2000, Singh and Fogler.pdf>," vol. 46, no. 5, pp. 1059–1074, 2000.

[4] N. V. Bhat and A. K. Mehrotra, "Measurement and prediction of the phase behavior of wax- solvent mixtures: Significance of the wax dis appearance temperature," *Industrial & engineering chemistry research*, vol. 43, no. 13, pp. 3451–3461, 2004.

[5] N. V. Bhat and A. K. Mehrotra, "Modeling of deposition from "waxy" mixtures in a pipeline under laminar flow conditions via moving boundary formulation," *Industrial & engineering chemistry research*, vol. 45, no. 25, pp. 8728–8737, 2006.

[6] A. K. Mehrotra, S. Ehsani, S. Haj-Shafiei, and A. S. Kasumu, "A review of heat-transfer mechanism for solid deposition from "waxy" or paraffinic mixtures," *The Canadian Journal of Chemical Engineering*, vol. 98, no. 12, pp. 2463–2488, 2020.

[7] S. Ehsani and A. K. Mehrotra, "Effects of shear rate and time on deposit composition in the cold flow regime under laminar flow conditions," *Fuel*, vol. 259, p. 116238, 2020.

[8] S. Haj-Shafiei, D. Serafini, and A. K. Mehrotra, "A steady-state heat-transfer model for solids deposition from waxy mixtures in a pipeline," *Fuel*, vol. 137, pp. 346–359, 2014.

[9] L. F. Azevedo and A. M. Teixeira, "A critical review of the modeling of wax deposition mechanisms," *Petroleum Science and Technology*, vol. 21, no. 3-4, pp. 393–408, 2003.

[10] P. Singh, R. Venkatesan, H. Scott Fogler, and N. R. Nagarajan, "Morphological evolution of thick wax deposits during aging," *AIChE Journal*, vol. 47, no. 1, pp. 6–18, 2001.

[11] K. G. Paso and H. S. Fogler, "Bulk stabilization in wax deposition systems," *Energy and Fuels*, vol. 18, no. 4, pp. 1005–1013, 2004.

[12] C. Sarica and M. Volk, "Tulsa University Paraffin Deposition Projects," no. February 2014, p. 130, 2004. [Online]. Available: http://www.osti.gov/servlets/purl/834175-PkzzCp/native/

[13] H. S. Lee, "Computational and Rheological Study of Wax Deposition and Gelation in Subsea Pipelines," p. 127, 2008.

[14] C. Van Der Geest, V. C. B. Guersoni, D. Merino-Garcia, and A. C. Bannwart, "Wax deposition experiment with highly paraffinic crude oil in laminar single-phase flow unpredictable by molecular diffusion mechanism," *Energy & Fuels*, vol. 32, no. 3, pp. 3406–3419, 2018.

[15] A. Aiyejina, D. P. Chakrabarti, A. Pilgrim, and M. Sastry, "Wax formation in oil pipelines: A critical review," *International journal of multiphase flow*, vol. 37, no. 7, pp. 671–694, 2011.

[16] H. M. Veiga, F. P. Fleming, and L. F. Azevedo, "Wax Deposit Thermal Conductivity Measurements under Flowing Conditions," *Energy and Fuels*, vol. 31, no. 11, pp. 11 532–11 547, 2017.

[17] F. P. Fleming, "Fundamental study of wax deposition under real flow conditions," no. April, p. 210, 2018.

[18] A. K. Mehrotra and N. V. Bhat, "Modeling the effect of shear stress on deposition from "waxy" mixtures under laminar flow with heat transfer," *Energy & fuels*, vol. 21, no. 3, pp. 1277–1286, 2007.

[19] N. V. Bhat and A. K. Mehrotra, "Modeling of deposit formation from "waxy" mixtures via moving boundary formulation: Radial heat transfer under static and laminar flow conditions," *Industrial & engineering chemistry research*, vol. 44, no. 17, pp. 6948–6962, 2005.

[20] C. Jiang, K. Zhao, C. Fu, and L. Xiao, "Characterization of morphology and structure of wax crystals in waxy crude oils by terahertz time-domain spectroscopy," *Energy & Fuels*, vol. 31, no. 2, pp. 1416–1421, 2017.

[21] M. Kane, M. Djabourov, J.-L. Volle, J.-P. Lechaire, and G. Frebourg, "Morphology of paraffin crystals in waxy crude oils cooled in quiescent conditions and under flow," *Fuel*, vol. 82, no. 2, pp. 127–135, 2003.

[22] M. Kurniawan, S. Subramanian, J. Norrman, and K. Paso, "Influence of Microcrystalline Wax on the Properties of Model Wax-Oil Gels," *Energy and Fuels*, vol. 32, no. 5, pp. 5857–5867, 2018.

[23] A. A. Soedarmo, N. Daraboina, and C. Sarica, "Validation of wax deposition models with recent laboratory scale flow loop experimental data," *Journal of Petroleum Science and Engineering*, vol. 149, pp. 351–366, 2017.

[24] S. Zheng, M. Saidoun, K. Mateen, T. Palermo, Y. Ren, and H. S. Fogler, "Wax deposition modeling with considerations of non-Newtonian fluid characteristics," *Proceedings of the Annual Offshore Technology Conference*, vol. 1, pp. 548–565, 2016.

[25] D. E. Andrade, M. A. M. Neto, and C. O. Negrão, "Non-monotonic response of waxy oil gel strength to cooling rate," *Rheologica Acta*, vol. 57, no. 10, pp. 673–680, 2018.

[26] S. Zheng, M. Saidoun, T. Palermo, K. Mateen, and H. S. Fogler, "Wax Deposition Modeling with Considerations of Non-Newtonian Characteristics: Application on Field-Scale Pipeline," *Energy and Fuels*, vol. 31, no. 5, pp. 5011–5023, 2017.

[27] C. Van Der Geest, V. C. B. Guersoni, D. Merino-Garcia, and A. C. Bannwart, "Rheological study under simple shear of six gelled waxy crude oils," *Journal of Non-Newtonian Fluid Mechanics*, vol. 247, pp. 188–206, 2017.

[28] J. P. Cabanillas, A. T. Leiroz, and L. F. Azevedo, "Wax deposition in the presence of suspended crystals," *Energy & Fuels*, vol. 30, no. 1, pp. 1–11, 2016.

[29] K. Paso, T. Kompalla, N. Aske, H. P. Rønningsen, G. Øye, and J. Sjöblom, "Novel surfaces with applicability for preventing wax deposition: A review," *Journal of Dispersion Science and Technology*, vol. 30, no. 6, pp. 757–781, 2009.

[30] W. Hayduk and B. Minhas, "Correlations for prediction of molecular diffusivities in liquids," *The Canadian Journal of Chemical Engineering*, vol. 60, no. 2, pp. 295–299, 1982.

[31] A. Matzain, "Multiphase flow paraffin deposition modeling." 2002.

[32] S. Haj-Shafiei, B. Workman, M. Trifkovic, and A. K. Mehrotra, "In-situ monitoring of paraffin wax crystal formation and growth," *Crystal Growth & Design*, vol. 19, no. 5, pp. 2830–2837, 2019.

[33] S. Correra, A. Fasano, L. Fusi, and D. Merino-Garcia, "Calculating deposit formation in the pipelining of waxy crude oils," *Meccanica*, vol. 42, no. 2, pp. 149–165, 2007.

[34] E. D. Burger, T. K. Perkins, and J. H. Striegler, "Studies of Wax Deposition in the Trans Alaska Pipeline." *JPT, Journal of Petroleum Technology*, vol. 33, no. 6, pp. 1075–1086, 1981.

[35] F. Jessen and J. N. Howell, "Effect of Flow Rate on Paraffin Accumulation in Plastic, Steel, and Coated Pipe," *Transactions of the AIME*, vol. 213, no. 01, pp. 80–84, 1958.

[36] J. S. Weingarten and J. A. Euchner, "Methods for Predicting Wax Precipitation and Deposition." *SPE Production Engineering*, vol. 3, no. 1, pp. 121–126, 1988.

[37] A. Hamouda and S. Davidsen, "An Approach for Simulation of Paraffin Deposition in Pipelines as a Function of Flow Characteristics With a Reference to Teesside Oil Pipeline," no. 1, 1995.

[38] R. Venkatesan and H. S. Fogler, "Comments on analogies for correlated heat and mass transfer in turbulent flow," *AIChE Journal*, vol. 50, no. 7, pp. 1623–1626, 2004.

[39] A. A. Soedarmo, N. Daraboina, and C. Sarica, "Microscopic Study of Wax Deposition: Mass Transfer Boundary Layer and Deposit Morphology," *Energy and Fuels*, vol. 30, no. 4, pp. 2674–2686, 2016.

[40] S. Ehsani and A. K. Mehrotra, "Validating heat-transfer-based modeling approach for wax deposition from paraffinic mixtures: An analogy with ice deposition," *Energy & fuels*, vol. 33, no. 3, pp. 1859–1868, 2019.

[41] H. M. Veiga, L. Boher e Souza, F. P. Fleming, I. Ibanez, R. C. Linhares, A. O. Nieckele, and L. F. A. Azevedo, "Experimental and numerical study of wax deposition in a laboratory-scale pipe section under well-controlled conditions," *Energy & Fuels*, vol. 34, no. 10, pp. 12 182–12 203, 2020.

[42] H. Bidmus and A. K. Mehrotra, "Measurement of the liquid- deposit interface temperature during solids deposition from wax- solvent mixtures under sheared cooling," *Energy & fuels*, vol. 22, no. 6, pp. 4039–4048, 2008.

[43] H. Bidmus and A. K. Mehrotra, "Measurement of the liquid-deposit interface temperature during solids deposition from wax-solvent mixtures under static cooling conditions," *Energy & fuels*, vol. 22, no. 2, pp. 1174–1182, 2008.

[44] N. Fong and A. K. Mehrotra, "Deposition under turbulent flow of wax- solvent mixtures in a bench-scale flow-loop apparatus with heat transfer," *Energy & fuels*, vol. 21, no. 3, pp. 1263–1276, 2007.

[45] A. S. Kasumu and A. K. Mehrotra, "Solids deposition from two-phase wax–solvent–water "waxy" mixtures under turbulent flow," *Energy & fuels*, vol. 27, no. 4, pp. 1914–1925, 2013.

[46] R. Tiwary and A. K. Mehrotra, "Deposition from wax- solvent mixtures under turbulent flow: Effects of shear rate and time on deposit properties," *Energy & Fuels*, vol. 23, no. 3, pp. 1299–1310, 2009.

[47] A. Fasano, L. Fusi, and S. Correra, "Mathematical models for waxy crude oils," *Meccanica*, vol. 39, no. 5, pp. 441–482, 2004.

[48] D. Dodge and A. Metzner, "Turbulent flow of non-newtonian systems," *AIChE Journal*, vol. 5, no. 2, pp. 189–204, 1959.

[49] S. Ravichandran, *Mechanistic Study of Wax Deposition-Effect of Super Saturation*. The University of Tulsa, 2018.

[50] H. Zhang, K. Lamnawar, and A. Maazouz, "Rheological modeling of the diffusion process and the interphase of symmetrical bilayers based on PVDF and PMMA with varying molecular weights," *Rheologica Acta*, vol. 51, no. 8, pp. 691–711, 2012.

[51] C. R. Wilke and P. Chang, "Correlation of diffusion coefficients in dilute solutions," *AIChE Journal*, vol. 1, no. 2, pp. 264–270, 1955.

[52] A. L. Sousa and H. A. Matos, "Correlations for prediction of molecular diffusivities in liquids at infinite dilution for normal paraffin solutions," *The Canadian Journal of Chemical Engineering*, vol. 98, no. 4, pp. 1031–1032, 2020. [Online]. Available: https://onlinelibrary.wiley.com/doi/abs/10.1002/cjce.23651

[53] Y. W. Wen and A. Kantzas, "Monitoring bitumensolvent interactions with low-field nuclear magnetic resonance and x-ray computer-assisted tomography," *Energy & Fuels*, vol. 19, no. 4, pp. 1319–1326, 2005. [Online]. Available: https://doi.org/10.1021/ef049764g

[54] A. Fayazi, S. Kryuchkov, and A. Kantzas, "Evaluating diffusivity of toluene in heavy oil using nuclear magnetic resonance imaging," *Energy & Fuels*, vol. 31, no. 2, pp. 1226–1234, 2017. [Online]. Available: https://doi.org/10.1021/acs.energyfuels.6b02464

[55] A. R. Mutina and M. D. Hürlimann, "Correlation of transverse and rotational diffusion coefficient: A probe of chemical composition in hydrocarbon oils," *Journal of Physical Chemistry A*, vol. 112, no. 15, pp. 3291–3301, 2008.

[56] W. Alizadeh, A.A., "Mutual diffusion coefficients for binary mixtures of normal alkanes," *Int. J. Thermophys.*, vol. 3, p. 307–323, 1982.

[57] M. A. Matthews and A. Akgerman, "Diffusion coefficients for binary alkane mixtures to 573 k and 3.5 mpa," *AIChE Journal*, vol. 33, no. 6, pp. 881–885, 1987. [Online]. Available: https://aiche.onlinelibrary.wiley.com/doi/abs/10.1002/aic.690330602

[58] J. B. Rodden, C. Erkey, and A. Akgerman, "High-temperature diffusion, viscosity, and density measurements in n-eicosane," *Journal of Chemical & Engineering Data*, vol. 33, no. 3, pp. 344–347, 1988. [Online]. Available: https://doi.org/10.1021/je00053a034

[59] J. W. Moore and R. M. Wellek, "Diffusion coefficients of n-heptane and n-decane in n-alkanes and n-alcohols at several temperatures," *Journal of Chemical & Engineering Data*, vol. 19, no. 2, pp. 136–140, 1974. [Online]. Available: https://doi.org/10.1021/je60061a023

[60] T. Zhan, Y. Su, Y. Zhang, X. Liu, and M. He, "Mutual diffusion coefficients of ethanol + n-heptane and diethyl carbonate + n-heptane from 288.15 k to 318.15 k," *The Journal of Chemical Thermodynamics*, vol. 144, p. 106089, 2020. [Online]. Available: http://www.sciencedirect.com/science/article/pii/S0021961419306081

[61] Y. Zhang, Z. TT, C. JS, and H. MG, "Mutual diffusion coefficients of 3-methyl-1-butanol + n-heptane and 2-methyl-1-butanol + n-heptane from 288.15 K to 318.15 K," *Journal of Chemical Thermodynamics*, vol. 131, pp. 97–103, 2019. [Online]. Available: https://www.cheric.org/research/tech/periodicals/view.php?seq=1703777

[62] H. Fadaei, J. M. Shaw, and D. Sinton, "Bitumen–toluene mutual diffusion coefficients using microfluidics," *Energy & Fuels*, vol. 27, no. 4, pp. 2042–2048, 2013. [Online]. Available: https://doi.org/10.1021/ef400027t

[63] A. Leahy-Dios and A. Firoozabadi, "Unified model for nonideal multicomponent molecular diffusion coefficients," *AIChE journal*, vol. 53, no. 11, pp. 2932–2939, 2007.

[64] A. Noorjahan, X. Tan, Q. Liu, M. R. Gray, and P. Choi, "Study of cyclohexane diffusion in athabasca asphaltenes," *Energy & Fuels*, vol. 28, no. 2, pp. 1004–1011, 2014. [Online]. Available: https://doi.org/10.1021/ef402312d

[65] B. Jacimovic, S. Genic, and D. Lelea, "Calculation of the Heat Transfer Coefficient for Laminar Flow in Pipes in Practical Engineering Applications," *Heat Transfer Engineering*, vol. 39, no. 20, pp. 1794–1800, 2018. [Online]. Available:

https://doi.org/10.1080/01457632.2017.1388949
[66] L. Syam Sundar and M. K. Singh, "Convective heat transfer and friction factor correlations of nanofluid in a tube and with inserts: A review," *Renewable and Sustainable Energy Reviews*, vol. 20, pp. 23–35, 2013. [Online]. Available: http://dx.doi.org/10.1016/j.rser.2012.11.041
[67] V. Gnielinski, "New equations for heat and mass transfer in the turbulent flow in pipes and channels," *STIA*, vol. 41, no. 1, pp. 8–16, 1975.
[68] T. H. Chilton and A. P. Colburn, "Mass Transfer (Absorption) Coefficients: Prediction from Data on Heat Transfer and Fluid Friction," *Industrial and Engineering Chemistry*, vol. 26, no. 11, pp. 1183–1187, 1934.
[69] H. Hausen, "Darstellung des warmeuberganges in rohren durch verallgemeinerte potenzbeziehungen," *Z. VDI Beih. Verfahrenstech*, vol. 4, no. 91, 1943.
[70] E. N. Sieder and G. E. Tate, "Heat transfer and pressure drop of liquids in tubes," *Industrial & Engineering Chemistry*, vol. 28, no. 12, pp. 1429–1435, 1936.
[71] B. Na and R. L. Webb, "Mass transfer on and within a frost layer," *International Journal of Heat and Mass Transfer*, vol. 47, no. 5, pp. 899–911, 2004.
[72] E. Ramirez-Jaramillo, C. Lira-Galeana, and O. Manero, "Modeling wax deposition in pipelines," *Petroleum Science and Technology*, vol. 22, no. 7-8, pp. 821–861, 2004.
[73] J. A. Svendsen, "Mathematical modeling of wax deposition in oil pipeline systems," *AIChE Journal*, vol. 39, no. 8, pp. 1377–1388, 1993.
[74] Z. Wang, Y. Xu, Y. Zhao, Z. Li, Y. Liu, and J. Hong, "Role of shearing dispersion and stripping in wax deposition in crude oil pipelines," *Energies*, vol. 12, no. 22, 2019.
[75] T. Davenport and V. Conti, "Heat transfer problems encountered in the handling of waxy crude oils in large pipelines," *Journal of the Institute of Petroleum*, vol. 55, no. 555, pp. 147–64, 1971.
[76] D. J. Needham, B. T. Johansson, and T. Reeve, "The development of a wax layer on the interior wall of a circular pipe transporting heated oil," *Quarterly Journal of Mechanics and Applied Mathematics*, vol. 67, no. 1, pp. 93–125, 2014.
[77] A. Sousa, H. Matos, and L. Guerreiro, "Wax deposition mechanisms and the effect of emulsions and carbon dioxide injection on wax deposition: Critical review," *Petroleum*, 2019.
[78] R. Banki, H. Hoteit, and A. Firoozabadi, "Mathematical formulation and numerical modeling of wax deposition in pipelines from enthalpy–porosity approach and irreversible thermodynamics," *International Journal of Heat and Mass Transfer*, vol. 51, no. 13-14, pp. 3387–3398, 2008.
[79] J. Yang, Y. Lu, N. Daraboina, and C. Sarica, "Wax deposition mechanisms: Is the current description sufficient?" *Fuel*, vol. 275, p. 117937, 2020.
[80] R. Hoffmann and L. Amundsen, "Single-phase wax deposition experiments," *Energy and Fuels*, vol. 24, no. 2, pp. 1069–1080, 2010.
[81] "Olga wax." [Online]. Available: https://www.software.slb.com/products/olga/olga-solids-management/wax<<accessedonMay,2020>>
[82] G. Giacchetta, B. Marchetti, M. Leporini, A. Terenzi, D. Dall'Acqua, L. Capece, and R. Cocci Grifoni, "Pipeline wax deposition modeling: A sensitivity study on two commercial software," *Petroleum*, vol. 5, no. 2, pp. 206–213, 2019. [Online]. Available: https://doi.org/10.1016/j.petlm.2017.12.007
[83] R. S. D. F. Jana, S., "A numerical method to compute solidification and melting processes," *Applied Mathematical Modelling*, vol. 31, p. 93–119, 2007.
[84] R. Albagli, L. Souza, A. Nieckele *et al.*, "Reynolds number influence on wax deposition," in *OTC Brasil*. Offshore Technology Conference, 2017.
[85] S. Ehsani, S. Haj-Shafiei, and A. K. Mehrotra, "Deposition from waxy mixtures in a flow-loop apparatus under turbulent conditions: Investigating the effect of suspended wax crystals in cold flow regime," *The Canadian Journal of Chemical Engineering*, vol. 97, no. 10, pp. 2740–2751, 2019.
[86] L. Fusi, "On the stationary flow of a waxy crude oil with deposition mechanisms," *Nonlinear Analysis, Theory, Methods and Applications*, vol. 53, no. 3-4, pp. 507–526, 2003.
[87] R. Mendes, G. Vinay, G. Ovarlez, and P. Coussot, "Modeling the rheological behavior of waxy crude oils as a function of flow and temperature history," *Journal of Rheology*, vol. 59, no. 3, pp. 703–732, 2015.
[88] H. P. Rønningsen, "Rheological behaviour of gelled, waxy north sea crude oils," *Journal of Petroleum Science and Engineering*, vol. 7, no. 3-4, pp. 177–213, 1992.
[89] E. J. Soares, R. L. Thompson, and A. Machado, "Measuring the yielding of waxy crude oils considering its time-dependency and apparent-yield-stress nature," *Applied Rheology*, vol. 23, no. 6, 2013.
[90] S. B. Clough, H. E. Read, A. B. Metzner, and V. C. Behn, "Diffusion in slurries and in non-Newtonian fluids," *AIChE Journal*, vol. 8, no. 3, pp. 346–350, 1962.
[91] S. Wang, E. D. von Meerwall, S.-Q. Wang, A. Halasa, W.-L. Hsu, J. Zhou, and R. Quirk, "Diffusion and rheology of binary polymer mixtures," *Macromolecules*, vol. 37, no. 4, pp. 1641–1651, 2004.
[92] S. Todi, "Experimental and modeling studies of wax deposition in crude oil carrying pipelines." 2005.
[93] E. Cussler, S. E. Hughes, W. J. Ward III, and R. Aris, "Barrier membranes," *Journal of membrane science*, vol. 38, no. 2, pp. 161–174, 1988.
[94] R. Aris, "On the permeability of membranes with parallel, but interconnected, pathways," *Mathematical Biosciences*, vol. 77, no. 1-2, pp. 5–16, 1985.
[95] A. A. Soedarmo, N. Daraboina, H. S. Lee, and C. Sarica, "Microscopic Study of Wax Precipitationi-Static Conditions," *Energy and Fuels*, vol. 30, no. 2, pp. 954–961, 2016.
[96] F. Alnaimat and M. Ziauddin, "Wax deposition and prediction in petroleum pipelines," *Journal of Petroleum Science and Engineering*, vol. 184, no. April 2019, p. 106385, 2020. [Online]. Available: https://doi.org/10.1016/j.petrol.2019.106385
[97] J. A. Coutinho, J. A. Lopes da Silva, A. Ferreira, M. R. Soares, and J. L. Daridon, "Evidence for the aging of wax deposits in crude oils by Ostwald Ripening," *Petroleum Science and Technology*, vol. 21, no. 3-4, pp. 381–391, 2003.
[98] G. Madras and B. J. McCoy, "Temperature effects during ostwald ripening," *The Journal of chemical physics*, vol. 119, no. 3, pp. 1683–1693,

2003.

[99] N. V. Bhat and A. K. Mehrotra, "Modeling the effect of shear stress on the composition and growth of the deposit layer from "waxy" mixtures under laminar flow in a pipeline," *Energy & Fuels*, vol. 22, no. 5, pp. 3237–3248, 2008. [Online]. Available: https://doi.org/10.1021/ef800277g

[100] S. Ehsani, S. Haj-Shafiei, and A. K. Mehrotra, "Experiments and modeling for investigating the effect of suspended wax crystals on deposition from'waxy'mixtures under cold flow conditions," *Fuel*, vol. 243, pp. 610–621, 2019.

[101] M. Li, J. Su, Z. Wu, Y. Yang, and S. Ji, "Study of the mechanisms of wax prevention in a pipeline with glass inner layer," *Colloids and Surfaces A: Physicochemical and Engineering Aspects*, vol. 123, pp. 635–649, 1997.

[102] M. Rashidi, B. Mombekov, M. Marhamati *et al.*, "A study of a novel inter pipe coating material for paraffin wax deposition control and comparison of the results with current mitigation technique in oil and gas industry," in *Offshore technology conference Asia*. Offshore Technology Conference, 2016.

[103] S. B. Pope, "Turbulent flows," 2001.

[104] H. Vehkamäki, *Classical nucleation theory in multicomponent systems*. Springer Science & Business Media, 2006.

[105] "Ledaflow® advanced transient multiphase flow simulator." [Online]. Available: http://www.ledaflow.com/wp-content/uploads/2019/10/LedaFlow-Engineering-Product-Sheet.pdf<<accessedonMay,2020>>

[106] "Flow assurance applications." [Online]. Available: https://alfasim.esss.co/applications/flow-assurance-applications/<<accessedonJune,2020>>

[107] L. Hovden, C. Labes-Carrier, A. Rydahl, H. Ronningsen, and Z. Xu, "Pipeline wax deposition models and model for removal of wax by pigging: Comparison between model predictions and operational experience." in *Abstracts of Papers of the American Chemical Society*, vol. 225. AMER CHEMICAL SOC 1155 16TH ST, NW, WASHINGTON, DC 20036 USA, 2003, pp. U936–U936.

[108] Z. Huang, S. Zheng, and H. S. Fogler, *Wax deposition: experimental characterizations, theoretical modeling, and field practices*. CRC Press, 2016.

[109] "Tupdp - tulsa university paraffin deposition projects." [Online]. Available: http://www.tupdp.utulsa.edu/<<accessedonJune,2020>>

[110] Z. Huang, H. S. Lee, M. Senra, and H. Scott Fogler, "A fundamental model of wax deposition in subsea oil pipelines," *AIChE Journal*, vol. 57, no. 11, pp. 2955–2964, 2011.

[111] "Mwp - the michigan wax predictor." [Online]. Available: http://cheresearch.engin.umich.edu/fogler/mwp.html<<accessedonJune,2020>>

[112] L. H. A. Mahir, "Modeling paraffin wax deposition from flowing oil onto cold surfaces," Ph.D. dissertation, University of Michigan, 2020.